MINIREVIEW

Changes in Arterial Smooth Muscle Contractility, Contractile Proteins, and Arterial Wall Structure in Spontaneous Hypertension (43802)

C. SUBAH PACKER[1]

Department of Physiology and Biophysics, Indiana University School of Medicine, Indianapolis, Indiana 46202–5120

Abstract. **Heart disease, stroke, and kidney failure are leading causes of death. Essential hypertension is the major predisposing risk factor of cardiovascular disease. Yet, after several decades of intensive investigation, the initiating causative mechanism of essential hypertension is still unknown. However, investigators in the field generally agree that an increased total peripheral resistance (TPR) is the fundamental hemodynamic disorder in essential hypertension. This review addresses the hypothesis that the increased TPR of essential hypertension is due to a defective mechanism in the contractility of arterial smooth muscle. Force-velocity and length-tension studies have shown that both caudal arterial muscle and mesenteric resistance arterial muscle from spontaneously hypertensive rats (SHR) can shorten more and faster than muscle from normotensive control Wistar-Kyoto rats (WKY). In addition, the SHR muscle relaxation rate is slower compared with the WKY muscle. These alterations in mechanical behavior of SHR arterial muscle appear to be primary to the high blood pressure since MK-421 (enalapril maleate)-treated SHR arterial muscle shows the same increased velocity of shortening, increased shortening ability, and decreased relaxation rate as the untreated SHR muscle. MK-421 is an angiotensin-converting enzyme blocker. SHR maintained on MK-421 treatment have normal blood pressures in spite of being of the genetically hypertensive strain. While these findings are encouraging, several other important issues supporting the hypothesis require resolution and warrant review. Firstly, structural alterations of blood vessel walls in hypertension cause the walls to thicken and encroach on the vessel lumens contributing to the increased TPR. Whether such wall thickening is the cause or consequence of high blood pressure has been controversial in the literature. In this report, data are presented from a study in which MK-421-treated SHR were utilized as a model of prehypertensive SHR. Light micrograph observations and morphometric analyses were made of cross-sections of mesenteric resistance arteries from SHR, MK-421-treated SHR, and WKY. Results show that the MK-421-treated SHR resistance arteries had media thicknesses and a number of smooth muscle cell layers that were significantly less than in the untreated SHR and not different from the WKY. Secondly, velocity of shortening is dependent on actomyosin ATPase activity, and, since maximum velocity**

[1] To whom requests for reprints should be addressed at Department of Physiology and Biophysics, Indiana University School of Medicine, 635 Barnhill Drive, Indianapolis, IN 46202–5160.

0037-9727/94/2072-0148$10.50/0

of shortening has been shown to be increased in SHR arterial muscle, it became necessary to know whether or not an increased actomyosin ATPase activity might be responsible. Therefore, data from a study of SHR and WKY caudal arterial myofibrillar ATPase activities are compared. Myofibrillar ATPase and ATP were reacted in the test tube and the P_i liberated was measured as an index of the ATPase activity. Results do indeed indicate an increased actomyosin ATPase activity in SHR arterial muscle. Thirdly, the mechanism responsible for increased actomyosin ATPase activity in SHR arterial muscle is addressed. Data are presented from urea glycerol gel and Western blot analyses of the regulatory myosin light chain (MLC_{20}) that show that the level of phosphorylation of the MLC_{20} is 2- to 3-fold higher in SHR compared with WKY arterial muscle when stimulated to the same degree. Increased MLC_{20} phosphorylation can account for the increased ATPase activity and increased contractility. Finally, possible explanations for the increased MLC_{20} phosphorylation in the hypertensive arterial muscle and the relevance of studies on SHR arterial muscle to human essential hypertension are discussed. [P.S.E.B.M. 1994, Vol 207]

The vast majority, greater than 90%, of hypertensive patients have essential or primary hypertension. Essential hypertension is defined as having diastolic pressures greater than 90 mm Hg and the elevation in pressure is of unknown cause. The value of 90 mm Hg was not chosen arbitrarily. While it is difficult to assign a value to blood pressure (BP) above which the BP should be considered high, several large-scale epidemiological studies of the last 15–20 years have shown that diastolic pressures above 90 mm Hg have deleterious effects on health and longevity (1).

Hypertension has been called the "silent killer." The individual with high blood pressure usually feels generally well and presents no obvious signs or symptoms of disease. However, hypertension by itself brings about arterial damage. The main target organs of such damage are the brain, eyes, heart, and kidneys. Disability ensues, and eventually so does death. Death in such patients usually occurs due to vascular accidents, coronary occlusion, left ventricular failure, or renal failure as outlined in Figure 1 (2).

Hypertensive disease has received much intensive research, yet we are still faced with finding an initiating causative mechanism. Looking for an initial cause is a very difficult task because there are so many mechanisms involved in BP control. Irving Page's mosaic model shown in Figure 2 makes this point rather well (3). The last 40–50 years of intense research into what the cause of essential hypertension might be, while not having answered the question, allow us at this time to simplify the problem by ruling out those mechanisms of BP control which have been shown to be unaltered, at least initially, in spontaneous hypertension.

Most investigators in the field agree that blood volume, blood viscosity, and cardiac output are generally not altered in early essential hypertension. In most cases of essential hypertension, plasma volume is either unchanged or is decreased. An inverse relationship between diastolic pressure and blood volume is likely a reflection of a general decrease in vascular capacity in essential hypertensives. Increased blood viscosity has been reported for patients with high renin hypertension, while hypertensive patients with normal or low renin have normal blood viscosity (4). This suggests that blood viscosity increases in hypertension when there is renal involvement in the etiology of the disease. Similarly, the study of Letcher *et al.* (5) suggests that any increase in viscosity is secondary to the primary defect in essential hypertension: "It may be that arteriolar vasoconstriction, by altering capillary hydrostatic forces and promoting hemoconcentration, may lead to elevated hematocrit and plasma protein concentrations and, thereby, any observed changes in blood viscosity." In at least 70% of borderline essential hypertensive subjects, and in all patients with long-established hypertension, the cardiac output and the viscosity of the blood are normal. If the cardiac output

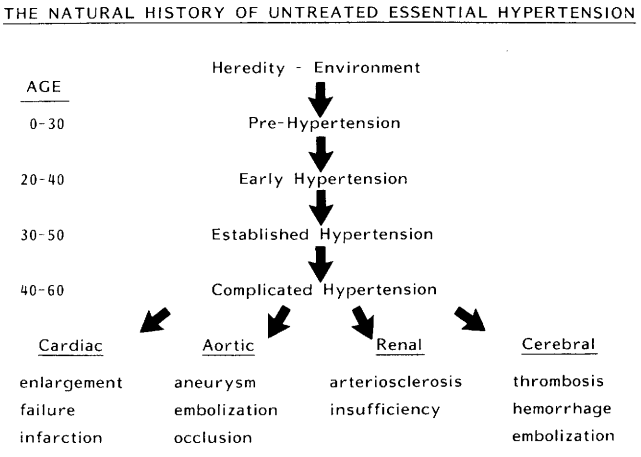

Figure 1. A representation of the natural history of untreated essential hypertension. Adapted from Figure 2–32 in Ref. 2, with kind permission from the author, N. M. Kaplan, and the copyright holder, Williams and Wilkins.

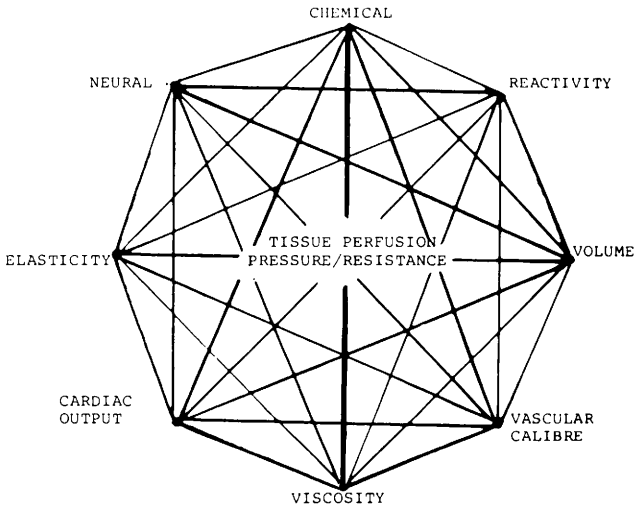

Figure 2. Diagram of the most important regulatory factors working in an interrelated manner to control blood pressure. Adapted from Figure 1 in Ref. 3, with kind permission from Beatrice Page on behalf of her husband, the author, Irvine Page, and from the copyright holder, The American Heart Association.

is lowered utilizing β-receptor blockers and atropine in the remaining 30% of subjects with borderline hypertension, peripheral vascular resistance rises, and the elevated pressure is maintained (6).

Most essential hypertensives (>80%) have normal renin, angiotensin II, aldosterone and Na^+ plasma levels (2). There was some evidence for a circulating natriuretic substance (7), but the experiments providing this evidence have not been consistently repeatable even by the original investigators. More recently, such a natriuretic factor has been characterized, but, while it has been shown to be involved in fluid volume and Na^+ homeostasis, it has apparently no effect on BP, glomerular filtration rate, or any other systemic haemodynamic mechanism (8). The theory was that if susceptible individuals eat more salt than their kidneys can handle, their blood volume will increase, thus stimulating release of natriuretic hormone. The hormone then inhibits the sodium pump of kidney tubules and facilitates salt excretion, but not enough to restore blood volume completely to normal. Although this should tend to lower the BP, at the same time, natriuretic hormone inhibits the pump in other types of cells, including those of smooth muscle in the arterioles, causing them to contract more readily thereby increasing BP. However, this theory requires increased Na^+ levels and increased blood volume, neither of which occurs in the majority of essential hypertensives.

Friedman (9) reported a decrease in net Na^+ efflux and an increased monovalent ion permeability in spontaneously hypertensive rat (SHR) vascular smooth muscle and red blood cells. It is now a basic part of Blaustein's theory that there is increased intracellular Na^+ concentration in hypertensive vascular smooth muscle cells. An increased intracellular Na^+ content would result in increased Na/Ca exchange and, therefore, an increased cytosolic free Ca^{2+} concentration resulting in increased vascular smooth muscle tonicity (10). While this has been an appealing explanation for essential hypertension, the evidence is contradictory and data of most studies are not supportive. Jones (11) reported an increased Na/K-ATPase activity that would offset an increased Na^+ leak. On the other hand, Haddy (12) reported that ouabain-sensitive ^{86}Rb uptake, a measure of Na/K pump activity, is suppressed. Tobian *et al.* (13, 14) suggested that in those predisposed to high BP, an increased accumulation of body Na^+ leads to increased vasoconstriction via hyper-reactivity of the sympathetic nervous system. This increased Na^+ accumulation was due to increased dietary Na^+ and decreased Na^+ excretion. Such an increased Na^+ retention would be followed by increased water retention, and Tobian felt that the thickened arterial walls seen in hypertensives was the result of hypertrophy due to swelling. However, there are many individuals on low Na^+ diets who become hypertensive and never have elevated Na^+ levels, and SHR do not require dietary Na^+ to initiate hypertension. Sympathectomy does not prevent hypertension, and hypertrophy of vascular smooth muscle in essential hypertension is known to be due to an increase in contractile proteins not to water accumulation (see Arterial Wall Structure in Hypertension below). Another point of interest is the report by Weinberger (15) that BP in SHR can be raised a maximum of only 10 mm Hg when utilizing massive Na^+ loading (600–800 mEq/day). Furthermore, an increased intracellular Na^+ concentration should result in an increase in membrane potential, but Steikel (16) reported that 4- to 5-week-old SHR and normotensive Wistar-Kyoto rats (WKY) have similar vascular smooth muscle membrane potentials, and shapes and positions of norepinephrine dose-response curves. Finally, as Postnov and Orlov (17) pointed out, the data on red blood cell Na^+ content in essential hypertension are contradictory, Na/Ca exchange is not likely to be greatly important in overall intracellular Ca^+ concentration regulation and evidence for an altered Na/Ca exchange in high blood pressure is lacking. Rather, the data generally suggest increased passive permeability, decrease in Ca^{2+}-binding ability, and decreased efficiency of Ca^{2+}-pump operation in the plasma membrane (18–22).

Neurogenic mechanisms of BP control have perhaps received the most investigative attention. However, the literature is full of contradictory results. There are reports that there is increased norepinephrine release, decreased release, increased reuptake, decreased reuptake, and no difference in either release or reuptake of norepinephrine in sympathetic nerves

of hypertensives (23–27). Most of the evidence supports the findings that sympathetic activity and adrenalin secretion are normal in the majority of hypertensives. In any case, it is unlikely that increased sympathetic activity alone will result in permanent hypertension. This latter conclusion is in accordance with findings in patients with duodenal ulcer disease, most of whom are normotensive in spite of an increased norepinephrine release which persists even after vagotomy. At any rate, whether the agonist be humoral or neural, it is the vessel calibre that ultimately decides the total peripheral resistance (TPR) and, given that cardiac output is constant, will determine the BP.

In reviewing the literature two facts stand out. One is that essential hypertension has a hereditary factor. Most essential hypertensive patients have family medical histories of hypertension. The essential hypertensive is born with a predisposition to developing hypertension. The other fact is that an increased TPR is the cardinal haemodynamic disorder in essential hypertension.

What might cause this increased TPR? The Poiseulle equation, $\dot{V} = \Delta P \pi r^4 / 8\eta L$ where: $\dot{V}$ = blood flow, ΔP = pressure gradient, r = vessel radius, L = vessel length and η = viscosity coefficient, reveals that blood viscosity and vessel geometry affect the resistance to flow. Since, as already stated, blood viscosity remains constant at least in early essential hypertension, then changes in resistance must be due to changes in tube geometry. Since flow varies directly and resistance inversely with the fourth power of the radius, blood flow and resistance are markedly affected by small changes in vessel calibre. Then, if flow remains constant due to relatively constant cardiac output, but resistance rises, BP must also rise. Based on this rationale, the important resulting question is: What causes a decrease in vessel calibre in early essential hypertension?

There is an increased wall/lumen ratio in hypertensive vessels, and it has been established that this increased wall/lumen ratio is due to hypertrophy and/or hyperplasia of vessel walls with encroachment on lumens (28–34). Whether hypertrophy, hyperplasia, or both processes occur depends on the particular vessel type. Hypertrophy followed by hyperplasia occurs in the larger muscular arteries while hyperplasia alone is responsible for changes in wall geometry of smaller resistance arteries (32, 33). However, there is still the important question as to whether or not increased TPR occurs prior to or secondarily to changes in blood vessel wall geometry in essential hypertension. There is much controversy in the literature regarding the answer to this question. The majority of studies report that the increased TPR does occur prior to changes in blood vessel wall geometry and suggest that high blood pressure triggers hypertrophy and/or hyperplasia of the media (34–37). These results indicate that the decreased radius thought to be responsible for the initial increase in resistance cannot be due to hypertrophied arterial walls.

Vascular smooth muscle reactivity may be altered in essential hypertensives. This could mean an increased contractile response due to altered smooth muscle contractility. Contractility is the muscle's ability to stiffen or to shorten and, therefore, involves force, velocity, length, and time. The thought, then, is that hypertensive arteries may narrow more and more rapidly, and possibly remain narrowed for prolonged periods in response to any given agonist. Either increased narrowing ability, prolonged narrowing, or both could result in increasing resistance and high blood pressure. Thickening of the arterial walls either accompanies or is caused by elevated BP. This results in a vicious cycle where hypertrophy and/or hyperplasia contribute to maintaining or further increasing high blood pressure as outlined in Figure 3.

Mechanical Properties of Arterial Smooth Muscle

Vascular muscle has two main functions: (i) to actively shorten resulting in vasoconstriction, and (ii) to increase vascular wall stiffness and thus resist distension. For all types of mammalian muscle, shortening velocity is maximal (V_{max}) at the optimal length (l_o) for maximum isometric tension development (P_o) (38, 39).

The relationship between load and velocity was described quantitatively by Hill's (40) hyperbolic equation $(P + a)(V + b) = b(P_o + a)$, where P = load, V = velocity of shortening, P_o = maximum isometric force, a = force constant, and b = velocity constant. However, the force-velocity (F-V) curves for both rat caudal arterial muscle and rat mesenteric resistance arterial muscle deviate from the hyperbola due to a reversal of curvature within 20% of the measured P_o values. Perhaps this is not so surprising, as

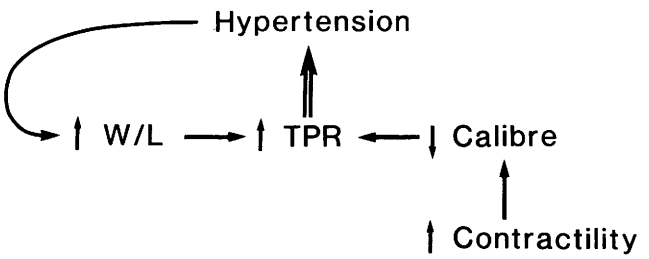

Figure 3. Diagram of one hypothesis for the causative mechanisms of essential hypertension. An increased arterial smooth muscle contractility (reactivity) results in increased vessel narrowing and resistance. Increased arterial resistance would be accompanied by a rise in blood pressure. Increased arterial wall/lumen ratios are thought to be secondary to the high blood pressure but, once these structural changes have occurred, would contribute to maintenance of hypertension.

these curves are qualitatively similar to those reported for single skeletal muscle fibre tetanic contractions and for cardiac twitch contractions (41–43). Figure 4 shows examples of *F-V* curves from cardiac, skeletal and caudal arterial smooth muscle, and a pressure-velocity curve from mesenteric arterial smooth muscle. Since the curves are not hyperbolic, the classical Hill equation cannot be fitted to this kind of data. The *F-V* relationship for arterial muscle carrying loads less than 80% P_o is exponential. Therefore velocities at zero load (V_{max}) can be derived by finding the intercept values for the exponential portions of the curves. Plotting velocity as a logarithmic function of all loads less than 80% P_o gives a straight line and the antilog value of the intercept at zero load gives V_{max} (34, 44). Values obtained from this type of analysis are comparable to V_{max} values reported for other arterial smooth muscles.

Reports have been published for various smooth muscle types including tracheal smooth muscle (45, 46) and vascular muscle (47, 48) that two cross-bridge cycling states operate during contraction. The mechanism hypothesized by Dillon *et al.* (47) was that the early phase of isotonic shortening was produced by phosphorylated cross-bridges cycling at a relatively rapid rate and that tonic stress maintenance was subserved by predominantly dephosphorylated cross-bridges that were non- or slow-cycling and that were termed "latch bridges." Dillon *et al.* (47) suggested that latch bridges act as an internal load on rapid-cycling bridges resulting in slow shortening of the muscle. Butler *et al.* (49) had postulated in 1976 that non-cycling bridges were present in resting smooth muscle, and these gave way to rapid-cycling cross-bridges in a tonic contraction. Siegman *et al.* (50) reported that the rate of energy utilization by cross-bridges was four times slower later in contraction than early in contraction. Similarly, Stephens and Skoog (51) had shown that oxygen uptake rate during the early phase of contraction in canine tracheal smooth muscle was three times faster than during the later phase. It has been concluded from these reports that shortening rate is greatest early in contraction and least late in contraction in smooth muscle and associated with a higher economy. This phenomenon is peculiar to smooth muscle, since tetanized skeletal muscle achieves maximum velocity of shortening early in contraction, and this velocity then remains constant until the onset of relaxation.

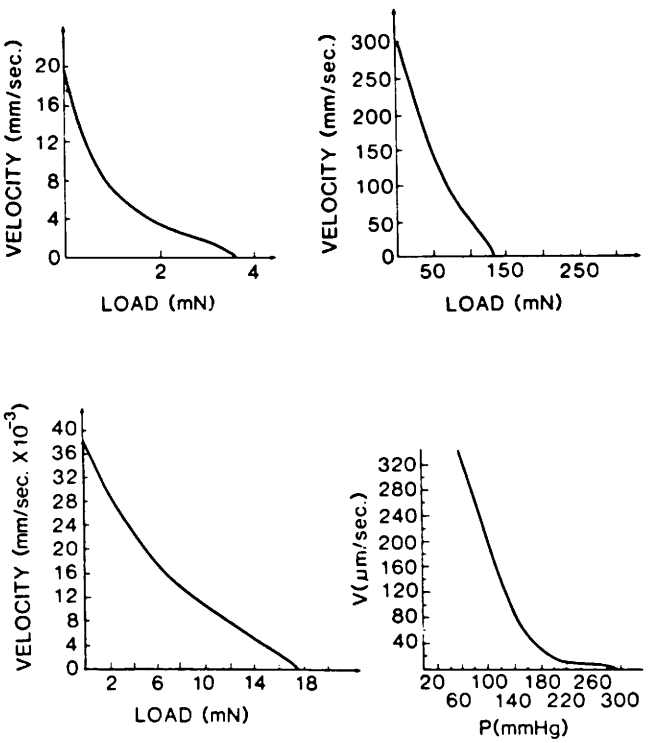

Figure 4. Illustrations of *F-V* curves from frog skeletal muscle fibre twitch contractions (n = 1), upper left-hand plot (41); canine cardiac muscle twitch contractions (mean curve), upper right-hand plot (43); rat caudal arterial smooth muscle strip tetanic contractions (n = 1), lower left-hand plot (75); and from rat mesenteric resistance arterial segment tetanic contractions (n = 1), lower right-hand plot (34). The skeletal fibre curve was obtained at a temperature between 1.35 and 2.5°C, while the cardiac and arterial muscle data were obtained at 37°C. Reprinted from Ref. 34, courtesy of the National Research Council of Canada.

Several explanations have been put forward to explain the nonhyperbolic *F-V* relationship. The drop from predicted velocity values at high loads has been thought to be due either to a decline in active state in cardiac muscle or to geometrical hindrances in skeletal fibres. Since tetanic contractions were used to obtain the nonhyperbolic (*F-V*) curves reported in skeletal and smooth muscle, it is unlikely that the steep drop in velocities at high loads is a function of diminished active state. A second possibility is that less sliding of filaments occurs than expected for a given load at loads approaching isometric load. At higher loads, there are shorter sarcomere lengths, and this results in greater side-to-side spacing of thick and thin filaments. Thus, less of the cross-bridge length is available for searching along (and around) the thin filaments decreasing the potential number of interactions between the myosin and actin filaments (41). A third possibility is provided by the discovery that there are two types of cross-bridge functional states operating in smooth muscle (47). These are the normal-cycling bridges recruited early in the contraction and are fairly rapidly replaced functionally by very slow-cycling latch bridges. Muscle carrying a heavier load must spend more time developing tension before it can shorten. It is quite possible that muscle shortening with loads approaching P_o are doing so with predominantly "slow" bridges which could account for the rapidly declining velocities seen at these loads. At heavier loads, the muscle spends a longer time in isometric mode, and

so the latch bridge phase commences prior to or very early into the shortening phase. However, this explanation fails to provide a rationale for the fact that in all muscle, both striated and smooth, the breakpoint in the *F-V* curve appears to occur at 78%–80% P_o regardless of the muscle type and any interventions imposed that alter maximum force and/or speed of shortening. Perhaps the best explanation for the biphasic nature of the *F-V* curves is the one put forth by Edman (42) more recently:

> The biphasic shape of the force-velocity relation may be an indication that the independent character of the cross-bridges is lost as the load on the muscle is raised above a certain level. That is, when the density of attached cross-bridges becomes high enough, this may impose some restriction upon the unattached bridges to find an appropriate binding site. In terms of A. F. Huxley's (52) cross-bridge model, these findings could therefore mean that the rate constant for attachment of cross-bridges is progressively reduced as the force exceeds 78% of its maximum value.

The maximum shortening velocities of various smooth muscles have been reported. These include canine airway (53), hog carotid artery (54), rat portal vein (55), rabbit and guinea pig taenia coli (39), guinea pig bladder (56), and rat caudal and mesenteric artery (34, 44). The V_{max} values reported for smooth muscle are 1/10 to 1/5 the values reported for skeletal and cardiac papillary muscle (57, 58) with vascular muscle being the slowest.

One reason suggested for the lower V_{max} in smooth muscle could be the relatively long time required to achieve full contraction because of the nature of the mechanisms of excitation-contraction coupling seen in smooth muscle (59). However, Barany (60) and Ruegg (61) have pointed out that, once contraction has begun, the velocity of shortening depends on the rate of splitting ATP. Differences in excitation-contraction coupling would account for differences in latent periods but not for differences in rates of contractile responses. Ruegg (61) and Murphy (62), among others, have provided evidence that the ATPase activity of smooth muscle contractile proteins is much less than that of skeletal muscle. Therefore, the lower activity of myosin ATPase in smooth muscle is a factor that contributes to the low maximum rate of smooth muscle shortening. The differences found in velocity between various mammalian smooth muscle types may be explained by the existence of isoforms of myosin. It is well established that isoenzymes exist in skeletal and cardiac muscle (63–65). More recently, the existence of at least two different heavy chains of myosin in several different smooth muscle tissues have been reported (66–70). In addition, several investigations have concluded that there are differences in isozyme patterns with altered smooth muscle states (71, 72).

Brutsaert, DeClerk *et al.* (73) have developed an analytical technique for studying relaxation which enables one to obtain insight into mechanisms of relaxation. Using cat heart papillary muscle (see inset to Fig. 5: upper panel), they have shown that the time course of relaxation is a function of the isometric load on the muscle. Brutsaert has termed this "load-dependent" relaxation. In frog ventricular muscle (see inset to Fig. 5: lower panel), on the other hand, relaxation is independent of load and appears to be controlled by the waning of the muscle's active state. They have termed this "inactivation-dependent" relaxation. The inactivation itself is dependent on the resequestration of calcium by the sarcoplasmic reticulum or its extrusion by the sarcolemma. Since frog ventricular muscle has a paucity of sarcoplasmic reticulum, the inactivation-dependent relaxation is understandable.

Johansson and Hellstrand (74) have studied relaxation in rat portal venous smooth muscle. Although

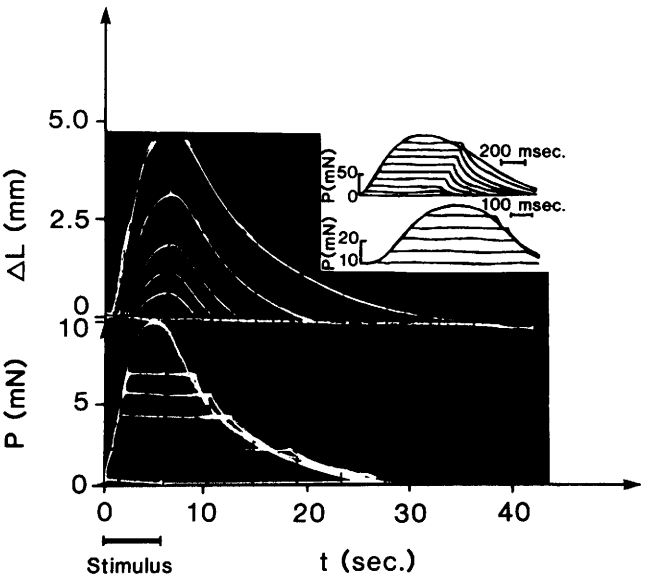

Figure 5. Photograph of actual recordings from an experiment of afterloaded contractions of rat caudal artery. Upper record: shortening traces at various afterloads. Lower record: tension traces at various afterloads with the greater loads corresponding to the simultaneous smaller changes in length seen in the upper record of the picture. Abscissa: the entire time sweep in all cases is 42 sec. The inset shows isometric tension versus time curves reprinted from Brutsaert *et al.* (73) for cat heart papillary (upper) and frog ventricular (lower) muscle. The upper set of curves shows that the onset of the isometric phase of relaxation occurs at different times for the different loads and the relaxation pathways all differ. This has been termed "load-dependent" relaxation by Brutsaert *et al.* (73). The lower set shows that the isometric relaxation pathway is the same for all loads. This has been termed "inactivation-dependent relaxation." Reprinted from Ref. 44, with permission from the National Research Council of Canada.

not specifically stated, it is evident from their reported curves that relaxation in this tissue is of the inactivation-dependent type. As can be seen in Figure 5, the rat caudal artery shows the same type of inactivation-dependent relaxation as reported for venous smooth muscle (75). Johansson and Hellstrand (74) have shown that differences in the time course of relaxation between isometric and isotonic responses in rat portal venous smooth muscle do not arise from any differences in electrical properties of cell membranes. With respect to the role of the excitation-contraction coupling mechanism, they considered that an increase in cell diameter during shortening might simply increase the average diffusion distances for efflux of calcium so that relaxation would be delayed. They also suggest as an alternative explanation, that the ability of the smooth muscle to carry a load over a relatively long period during isotonic relaxation may be attributed to the characteristics of the instantaneous *F-V* relations in the force range above P_o.

The load-dependent relaxation of arterial and venous smooth muscle is similar to that reported for frog ventricular muscle (73). However, the relaxation behavior of these smooth muscle preparations contrasts with the load-dependent behavior described for mammalian cardiac muscle (73). The ability, during isotonic lengthening, to sustain a load at "supra-isometric" levels is present at all loads in the smooth muscle and not merely limited to contractions at heavy afterloads as reported in mammalian cardiac muscle or to those at intermediate loads as seen in frog cardiac muscle. In contrast with smooth muscle, increasing the load during contraction does affect the isotonic relaxation phase of cat heart papillary muscle, and most markedly if the load clamp is applied during the last third of the shortening phase (73). Upon applying the heavier load there is initially a rapid elastic extension. In smooth muscle, when the load is applied early the elastic elongation phase is followed by redevelopment of shortening. However, at later times, approaching the summit of the shortening curve, the elastic phase is followed by a slower lengthening phase which then fuses smoothly with a subsequent more rapid phase (Fig. 5) (75). In contrast, the delayed extension in mammalian cardiac muscle consists of an initial slow and subsequent fast phase (73). There is some indirect evidence that it is the relatively poorly developed calcium sequestering mechanism of smooth muscle that is responsible for the inactivation-dependent relaxation seen in the venous and arterial smooth muscle preparations studied. Cardiac cells that normally show load-dependent relaxation display relaxation that is insensitive to load when pretreated with Brij 58 (76). Brij 58 acts by destroying the sarcoplasmic reticulum. Smooth muscle cells have a less well-developed sarcoplasmic reticulum than cardiac muscle cells. Most of the activating calcium would be derived from the transsarcolemmal calcium current during membrane depolarization of smooth muscle. Relaxation might then be expected to be related to the efflux of calcium ions across the sarcolemma. However, it must also be remembered that smooth muscle displays high viscosity behavior. Viscous forces, independent of the calcium mechanisms, can partly explain inactivation-dependent relaxation. Viscous forces would tend to delay isotonic lengthening and this delay would be more marked with smaller than with larger afterloads. Inactivation dependence could result from a slower detachment of force-generating sites in smooth muscle than that which is seen with cardiac or skeletal muscle. The high viscosity behavior of smooth muscle has been ascribed to specific physical interactions but could also be explained by slow dissociation of the dephosphorylated cross-bridges in smooth muscle (77).

Maximum isometric tension (P_o) development is of importance in that this parameter will give insight into the number of force-generating sites per cross-sectional area of muscle. Vascular smooth muscle characteristically develops relatively high forces over a wide range of lengths. Due to stiffness of passive parallel elastic elements, smooth muscles cannot normally be stretched to a length sufficient to reduce active force to zero, although longitudinal strips of the rabbit portal mesenteric vein show little or no active response when stretched to 1.4–1.7 l_o (78). Most smooth muscle preparations do not appear sensitive to "overstretch" but some irreversible loss of force-generating capacity has been observed at lengths above 1.25 l_o (79).

Mesenteric arterial muscle does not differ from other smooth muscle types with respect to the stiffness of passive parallel elastic elements (Fig. 6). However, the active force in this preparation approaches zero within 1.1–1.2 C_o (optimal circumference for P_o development; analogous to l_o for strip preparations). These latter findings point out the importance of working with the muscle at l_o when doing comparative studies of force-generating ability. While it may seem surprising that the rise in passive tension and the decrease in active tension are steep when mesenteric arterial muscle is stretched to only 1.1–1.2 l_o, it must be realized that the transmural pressure required to cause this small amount of stretch in these resistance vessels is very high (>210 mm Hg). Since these resistance arteries are mostly concerned with narrowing in order to control blood flow and considering that this function is normally performed *in vivo* at pressures usually less than 100 mm Hg, it may not be so surprising after all that the ability to produce active tension is lost at these high transmural pressures. The function of the arterial walls at high transmural pressure is to stiffen to resist

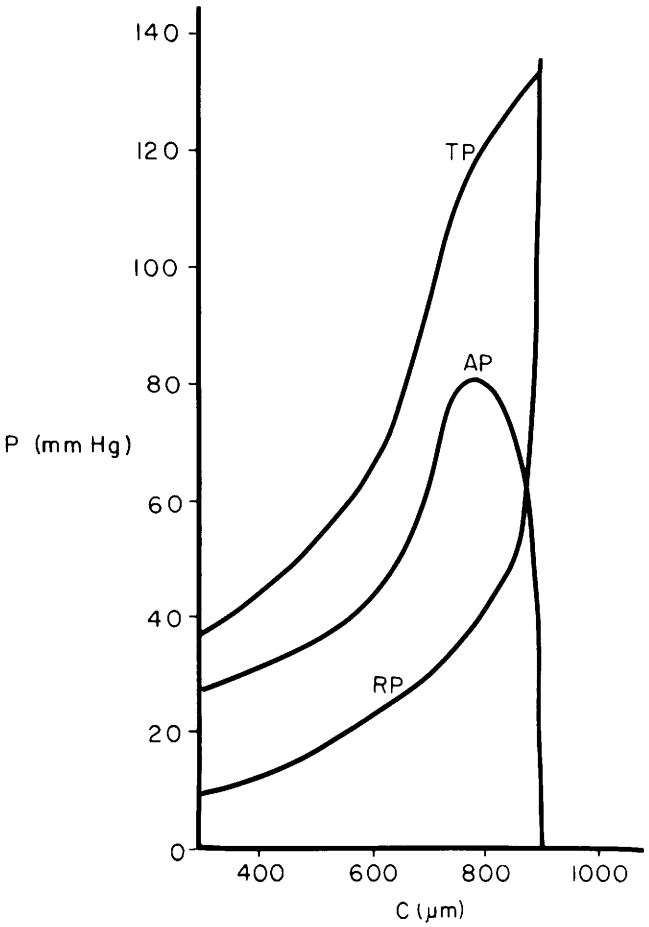

Figure 6. Pressure-circumference (*P-C*) curves for one WKY mesenteric artery experiment. This is an example of typical *P-C* curves obtained for mesenteric arteries where TP is the total pressure curve, RP is the resting pressure curve, and AP is the derived active pressure curve. Optimal circumference (C_o) was identified for each vessel studied as that circumference at which maximum active pressure could develop. Identification of C_o is essential to the normalization of all data. Reprinted from Ref. 82, with permission from the National Research Council of Canada.

further distension. The mesenteric arteries have the ability to do this via passive elements alone. Active shortening of contractile elements in distended intact arterial segments may actually cause slackening of passive elements and thus reduction of the contribution made by the passive elements to the net stiffness of the wall.

Mechanical Behavior of Hypertensive Arterial Smooth Muscle

The passive mechanical properties of SHR and WKY arterial smooth muscle do not appear to be significantly different from one another. This is based on the facts that SHR and WKY l_o for caudal arterial strips and C_o for mesenteric resistance arterial segments are not different, and on the fact that SHR, MK-421 (N-[(S)-1-(ethoxycarbonyl)-3-phenylpropyl]-L-Ala-L-Pro)-treated (MK-421 trt) SHR, and WKY passive tension-circumference curves for mesenteric resistance arteries are superimposable as shown in Figure 7 (34, 44). MK-421 (enalapril maleate) is an angiotensin I-converting enzyme (ACE) blocker, and MK-421 trt SHR serve as models of prehypertensive SHR. Others have reported similar passive length-tension curves for SHR and WKY arterial muscle (28, 80).

Prolonged isometric relaxation indicates that hypertensive vessels remain stiffer for longer periods than do the normotensive vessels. Prolonged isotonic relaxation would indicate that hypertensive vessels remain narrowed for prolonged periods. Such prolonged narrowing would contribute to an increase in TPR and thus to high blood pressure. Mechanical disturbances in the ability of hypertensive vascular smooth muscle to relax have been shown. Decreased extent of isometric relaxation in thoracic aorta of SHR has been shown (36, 81). This decreased relaxation persisted even after the hypertension had been controlled with medication (81). SHR and WKY caudal arterial muscle relax in a qualitatively similar manner, both showing inactivation-dependent relaxation (75). However, quantitative analysis shows slower relaxation rates for both isometric and isotonic contractions in SHR caudal arterial muscle. Similarly, SHR isobarically contracted mes-

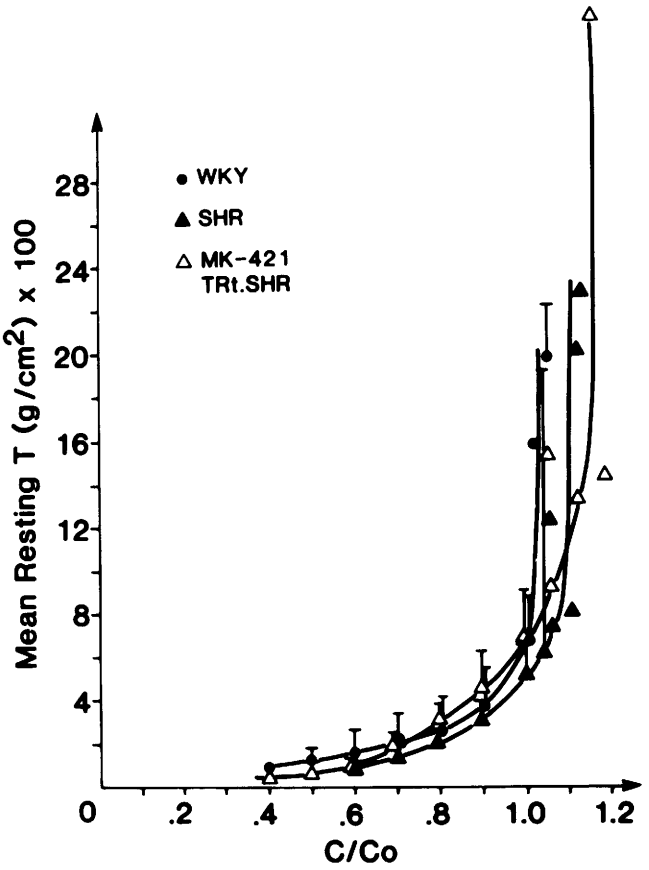

Figure 7. Illustrations of the mean SHR (n = 5), mean WKY (n = 5) and mean MK-421 trt SHR (n = 5) mesenteric arterial resting T-C/C_o curves. Reprinted from Ref. 34, courtesy of the National Research Council of Canada.

enteric resistance arterial segments are slower to relax than are WKY segments. Furthermore, untreated SHR and MK-421 trt SHR vessels show the same decreased relaxation rate as seen in Figure 8 (82). This indicates that the decreased relaxation rate is independent of the hypertension in this strain of genetically hypertensive rat. Although the underlying mechanisms have not been determined, an increased Ca^{2+} permeability (83), a decreased calcium resequestering rate, slower calcium extrusion from the cell (18), or a decreased myosin phosphatase activity (84) could be contributors to the observed prolonged relaxation.

Some investigators have found an increased P_o in SHR vascular smooth muscle (29), while others have found P_o decreased in hypertensives (85). Still others have found no differences between SHR and WKY P_o values (34, 44, 86, 87). The reports on SHR vascular smooth muscle P_o may not be as contradictory as they appear initially. Changes in P_o may occur as a result of vascular smooth muscle hypertrophy and/or hyperplasia in which an increase in the number of smooth muscle cells or in actin and myosin content in proportion to total arterial wall tissue has occurred. This has been reported to be the result in thickened SHR arterial walls (28, 88). One then would not expect to see increased P_o in younger rats. On the other hand, this may be a doubtful explanation since 19-week-old SHR, WKY, and MK-421 trt SHR mesenteric resistance arterial muscle show no difference in maximum tension (T_{max}) development despite the fact that the SHR arteries show significantly increased wall thicknesses over both the MK-421 trt SHR and the WKY vessels (34). In the latter study, no correlation could be made between hypertrophy and P_o. One must also keep in mind that an absolute increase in myosin with hypertrophy may be misleading in light of the reports of contractile protein isoform switches and phenotypic changes in hypertrophied or hyperplastic smooth muscle (89–91).

There are reports that vessels from SHR over eight weeks of age show significantly increased wall/lumen ratios (88). Yet there are reports that P_o is unchanged in SHR at 16 to 21 weeks of age as seen in Figures 9 and 10 (34, 44). No difference in P_o at 16 weeks may indicate that hypertrophy is not yet great enough to show the results of increased actin and myosin per cell or per cross-sectional area of media. There is some evidence in the literature to support the speculation that SHR vascular smooth muscle P_o may increase with advancing age. For instance, a decreased P_o was reported for 11- to 14-week-old SHR (85). No difference was found in P_o for 16- to 21-week-old SHR (34, 44), while an increased P_o was reported for 20- to 25-week-old SHR (88).

Yet there is also evidence that increased vascular

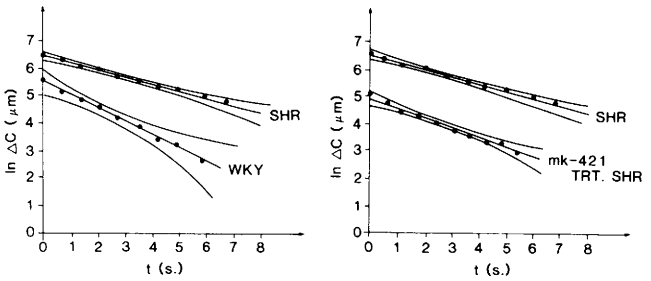

Figure 8. Plots of the mean SHR, mean WKY, and mean MK-421-treated SHR semilogarithmic ΔC (μm) vs t (sec) for contractions at 90 mm Hg pressure and their respective 95% confidence intervals for the means. The equations for SHR, WKY, and MK-421-treated SHR mean curves are $\ln \Delta C$ (μm) = a_{SHR} + [$slope_{SHR} \times t$ (sec)], $\ln \Delta C$ (μm) = a_{WKY} + [$slope_{WKY} \times t$ (sec)] respectively. It can be seen that the SHR curve is shifted above the WKY and the MK-421-treated SHR curves indicating that the SHR arteries have made a greater change in circumference (narrowed more) than either the WKY or the MK-421 treated SHR vessels. It can also be seen that the mean WKY slope is steeper than either the SHR or the MK-421-treated SHR slopes. The greater rate constant of the dilating or relaxation phase of the WKY contractions indicates that the narrowed SHR and MK-421-treated SHR vessels return to resting circumference at a slower rate than do the WKY vessels. Reprinted from Ref. 82, courtesy of the National Research Council of Canada.

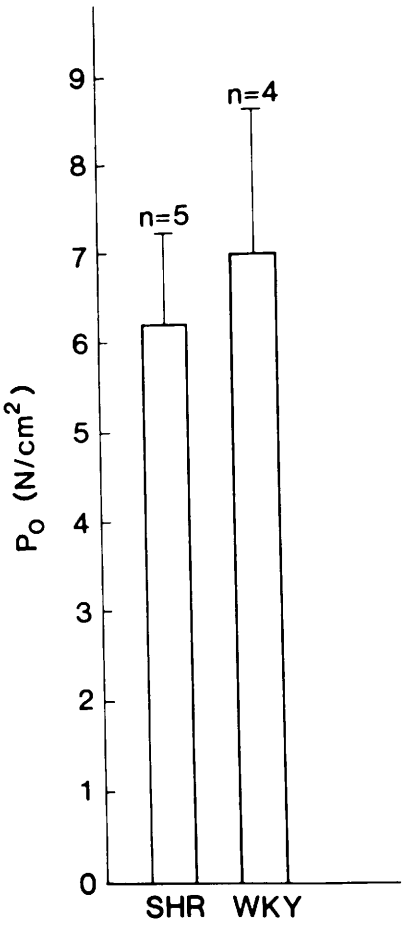

Figure 9. A bar graph comparing the mean SHR (n = 5) P_o and the mean WKY (n = 4) P_o values for caudal arterial smooth muscle. P_o is expressed in newtons per square centimetre. Reprinted from Ref. 75, courtesy of the National Research Council of Canada.

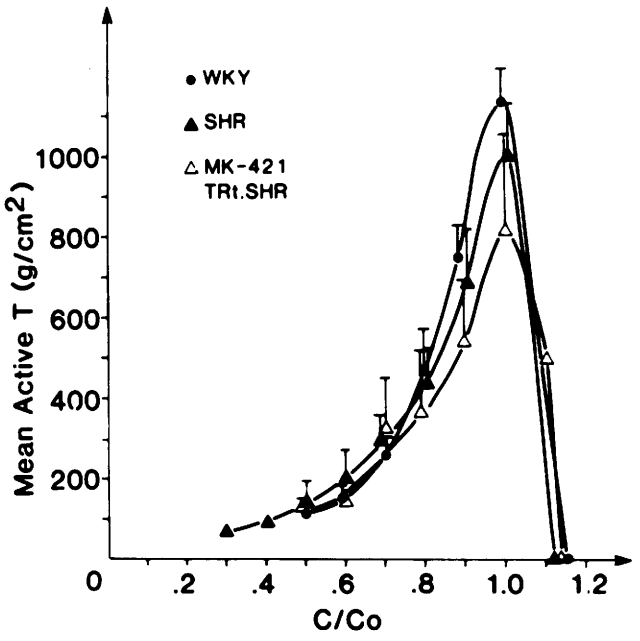

Figure 10. Illustrations of the mean SHR (n = 5), mean WKY (n = 5), and mean MK-421-treated SHR (n = 5) mesenteric arterial derived active T-C/C_o curves. There is no difference between the three curves indicating no difference in tension developing ability of hypertensive resistance arterial muscle compared with controls. Reprinted from Ref. 34, with permission from the National Research Council of Canada.

distending pressure-induced hypertrophy in vascular smooth muscle results in an increase in intermediate filaments and a coincidental decrease in myosin per actin ratio (92). This decreased myosin/actin ratio would likely result in a fall in P_o rather than an increased P_o with hypertrophy. Finding no difference in P_o at 16 to 21 weeks, then, might reflect a decline in P_o with increasing hypertrophy, from a once elevated value.

When carrying the same load, the SHR caudal arterial smooth muscle displays a greater degree of shortening than that of the WKY as seen in Figure 11 (44). Increased narrowing results in decreased lumen radius and thus results in increased resistance. While the degree of shortening in this particular type of smooth muscle (caudal arterial) is not great, a maximum shortening of 9% l_o with loads of 0.1 P_o will result in a 9% decrease in vessel radius which would increase resistance by about 50%. Previous theoretical consideration suggested a doubling of resistance with a 10% degree of smooth muscle shortening (93). Therefore, a 9% *in vitro* arterial smooth muscle shortening implicates physiologically significant changes in TPR and blood pressure. Probably of greater impact with regard to TPR and BP is the finding that isobarically contracting SHR mesenteric resistance arteries narrow to a significantly greater extent than do WKY resistant arteries when narrowing against the same given transmural pressures (34).

The SHR mesenteric arteries are also able to constrict to a significantly greater degree than the MK-421 trt SHR and WKY arteries for pressures ranging from 20 to 120 mm Hg as seen in Figure 12 (34). Interestingly, these differences in SHR arterial behavior are found for pressures in the normal physiological range. It can also be seen that SHR arteries are able to constrict against pressures well above the normal range (i.e., 120–310 mm Hg), while the WKY and MK-421 trt SHR arteries are unable to narrow against pressures greater than 210 and 240 mm Hg, respectively.

The increased ability of the SHR, mesenteric resistance arteries to constrict is probably due to the fact that SHR arterial velocities of shortening are significantly faster than the velocities of MK-421 trt SHR and WKY arteries. The derived SHR V_{max} is significantly faster than the MK-421 trt SHR and WKY V_{max}, which are not different from one another as seen in Figure 13 (34). It would seem that the antihypertensive MK-421 treatment was able to reverse or prevent the increased velocities of shortening seen in the SHR arterial smooth muscle to a significant extent and thus prevented the increased narrowing seen in the SHR vessels. Since the normotensive MK-421 trt SHR arteries do not show the same significantly increased narrowing as do the SHR arteries, it is still questionable as to whether or not the high blood pressure is primary or secondary to the increased narrowing in the hypertensive arteries. However, it is notable that the normotensive MK-421 trt SHR arteries display significantly faster velocities of narrowing than do the normotensive WKY arteries for pressures ranging from 20 to 120 mm Hg. The significance of this latter finding is that velocities of narrowing are faster in genetically hypertensive arteries and this intrinsic property of genetically hypertensive arterial smooth muscle may be interfered with by MK-421 treatment. Enalapril maleate is an antihypertensive drug that is eleven times more potent in lowering BP than is captopril despite having equal efficacy in reducing angiotensin II and therefore must have activities yet unknown in addition to ACE inhibition (94).

The tension-velocity (T-V) study of mesenteric resistance arteries produced velocity results in agreement with a previous F-V study of SHR and WKY caudal arterial strips. F-V analysis shows that the SHR caudal arterial strips shorten with greater velocity than WKY preparations as seen in Figure 14 (44). An increased V_{max} indicates an increased rate of actomyosin ATP hydrolysis. This may mean an elevated level of ATPase activity in hypertension due to changes in the intrinsic properties of the actomyosin ATPase, increased myosin light chain phosphorylation and/or an increased calcium concentration, as it has been shown for smooth muscle that an increased calcium concentration causes an increased ATPase activity (95).

The fact that there is some controversy in the lit-

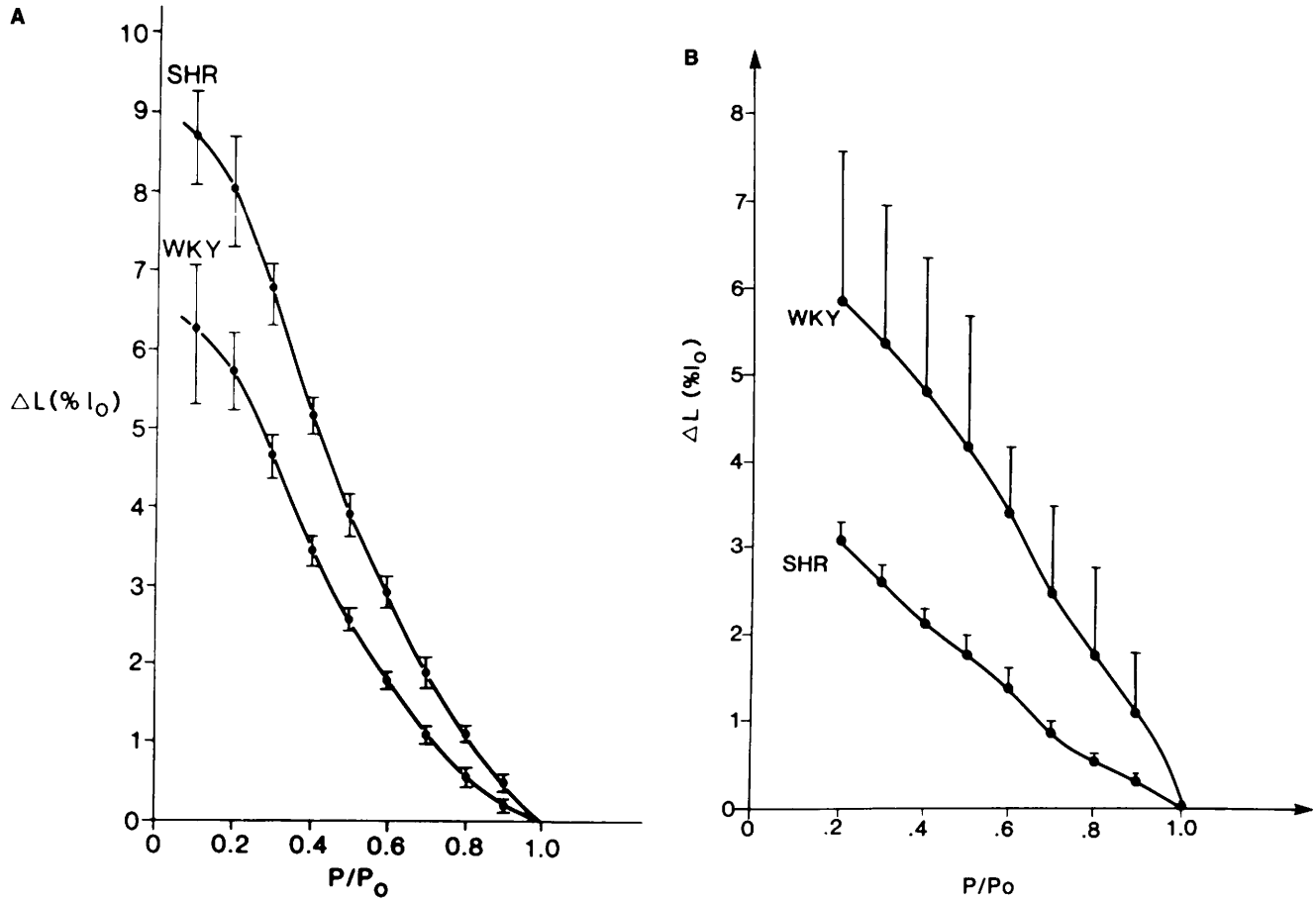

Figure 11. Panel A: The mean SHR (n = 6) and mean WKY (n = 5) caudal arterial smooth muscle ΔL (percent l_o) versus P/P_o curves from 16- to 18-week-old rats are compared. Reprinted with permission from Ref. 75, courtesy of the National Research Council of Canada. Panel B: The mean SHR (n = 7) and the mean WKY (n = 5) ΔL (percent l_o) versus P/P_o curves from 28- to 31-week-old rats are compared. Shortening ability of the arterial muscle is enhanced in SHR under 18 weeks of age but actually becomes impaired with aging and/or longer exposure to high transmural pressure and with hypertrophy.

erature regarding results of F-V studies of SHR arterial smooth muscle deserves some comment. While Packer and Stephens (34, 44) report an increased V_{max} in caudal and mesenteric resistance arterial muscle, Arner and Uvelius (87) found no difference in V_{max} between segments of abdominal aorta from SHR and WKY rats, and Mulvany (96) reported no difference in V_{max} for SHR and WKY mesenteric resistance arteries. This discrepancy between V_{max} results may be attributable to the different muscle preparations (e.g., caudal artery versus abdominal aorta) or to the difference in age range of the rats utilized in the various studies (e.g., 16 vs 20–25 weeks). Differences in V_{max} may reflect a change in Ca^{2+} concentrations and/or in levels of myosin light chain phosphorylation in response to agonists. Some light has been shed on this problem. The F-V studies reported previously for 16- to 19-week-old SHR and WKY caudal arterial strips were repeated on 28- to 31-week-old SHR and WKY preparations (97). In comparing the results of the F-V studies done on caudal arterial smooth muscle from 16- to 18-week-old SHR and WKY rats (Fig. 14) with the results of similar F-V studies done on caudal arterial smooth muscle from 28- to 31-week-old SHR and WKY rats (Fig. 15), the following was concluded: velocity of shortening is faster in caudal arterial smooth muscle from 16- to 18-week-old SHR compared with 16- to 18-week old WKY caudal arterial strips, but is significantly depressed in 28- to 31-week-old SHR compared with 28- to 31-week-old WKY preparations. The decrease in SHR V_{max} from once elevated speeds is not due simply to aging, for if this were the case, the WKY V_{max} should also have declined with age and the relative difference between SHR and WKY F-V curves seen in younger rats would not have been obliterated when comparing the older rats.

The disappearance of a difference in V_{max} between SHR and WKY caudal arterial smooth muscle may be due to a decline in SHR V_{max} due to hypertrophy of these hypertensive arteries, while the V_{max} of the WKY animals may show little or no change with age as there would be little or no hypertrophy in the arterial walls of these normotensive rats. That the media of blood vessels in hypertensives is thickened is well established (28–30, 34). Hypertrophy of smooth muscle cells in muscular arteries of older SHR rats may be

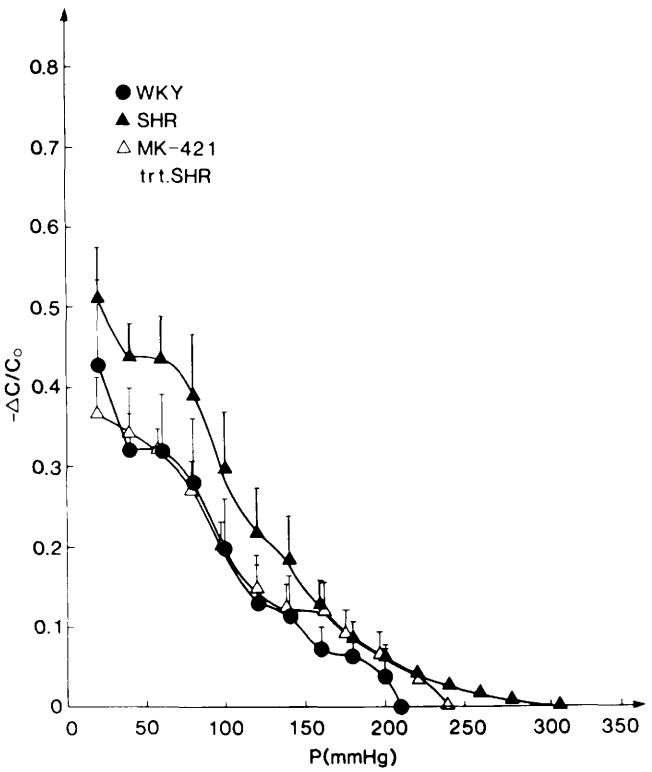

Figure 12. The mean active internal circumference responses as functions of transmural pressure ($-\Delta C/C_o$ – P mm Hg) for arteries from SHR (n = 5), WKY (n = 5), and MK-421-treated SHR (n = 5) are compared. Reprinted from Ref. 34, courtesy of the National Research Council of Canada.

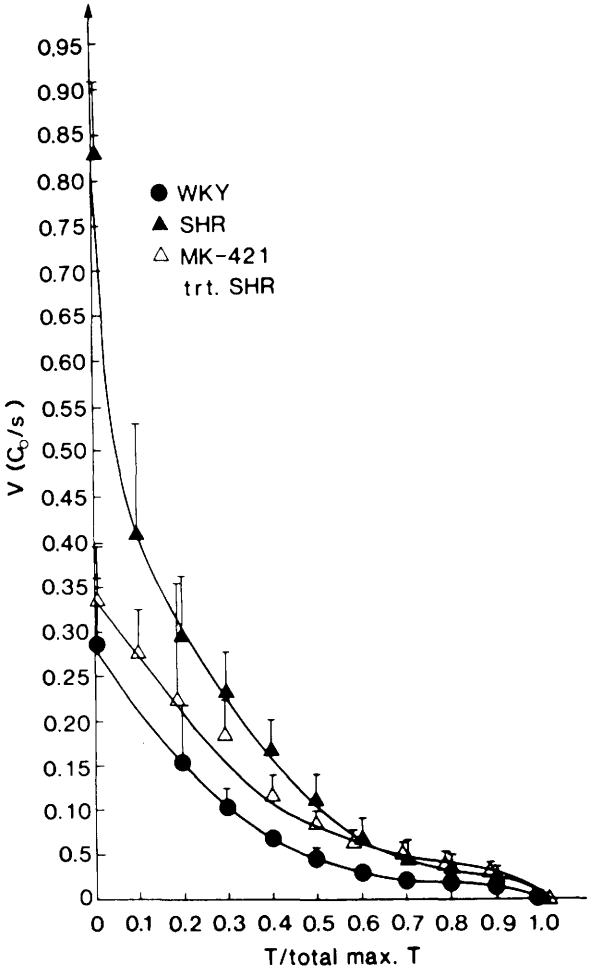

Figure 13. Mean SHR (n = 5), WKY (n = 5), and MK-421-treated SHR (n = 5) mesenteric arterial T/total maximum T-V curves are presented. Both the SHR and MK-421-treated SHR curves are elevated above the WKY curve for the lower loads ranging from 0 to 0.4 T/total maximum T values. However the treated SHR curve is also lower than the SHR curve indicating that either MK-421 treatment interferes with the faster velocity of genetically hypertensive vascular muscle or that the high transmural pressure of the untreated SHR has further enhanced the already faster velocity of the SHR arterial muscle. Reprinted from Ref. 34, courtesy of the National Research Council of Canada.

related to the effect of long duration of elevated blood pressure in these rats (33, 92, 93). Pressure-induced hypertrophy of arterial smooth muscle may not be unlike the pressure overload-induced hypertrophy of cardiac muscle. In such hypertrophied myocardium, a 25%–34% reduction in the velocity of shortening and depressed ATPase activity have been reported (98, 99). Since it is known that different myosin isoenzymes exist in smooth muscle, it may be speculated that the mechanism for the depressed V_{max} is due to depressed ATPase activity in hypertrophied hypertensive arterial smooth muscle as is the case in hypertrophied cardiac muscle (65, 99). On the other hand, the decrease in ATPase activity may not be linked to isozymes. For example, regulation of myosin light chain (MLC_{20}) phosphorylation may be altered in the hypertrophied arterial muscle. (See Contractile Protein Changes in Hypertensive Arterial Muscle below.)

It is more difficult to speculate as to the drastic drop in shortening ability in SHR arterial smooth muscle with age. There is evidence in the literature that increased vascular distending pressure-induced hypertrophy in vascular smooth muscle results in an increase in intermediate filaments (92). An increase in intermediate filaments may hinder shortening. At any rate, such loss of narrowing ability might in fact have a life-saving, partially compensating effect in established hypertension where hypertrophied vasculature alone can cause increased resistance and maintain high blood pressure.

A change in the relative numbers of cross-bridges undergoing fast or slow cycles has been demonstrated in smooth muscle. Early in contraction the majority of cross-bridges cycle rapidly while later in contraction the relative numbers of fast to slow cycling bridges decreases. The latter has been termed the "latch" phase and is thought to be a function of time or change in cell calcium concentration (45, 47, 48). Therefore, it is no longer adequate to report only parameters of smooth muscle mechanical behavior obtained in the classical way. Investigation of the mechanics of the early and late cross-bridge cycles in hypertensive ar-

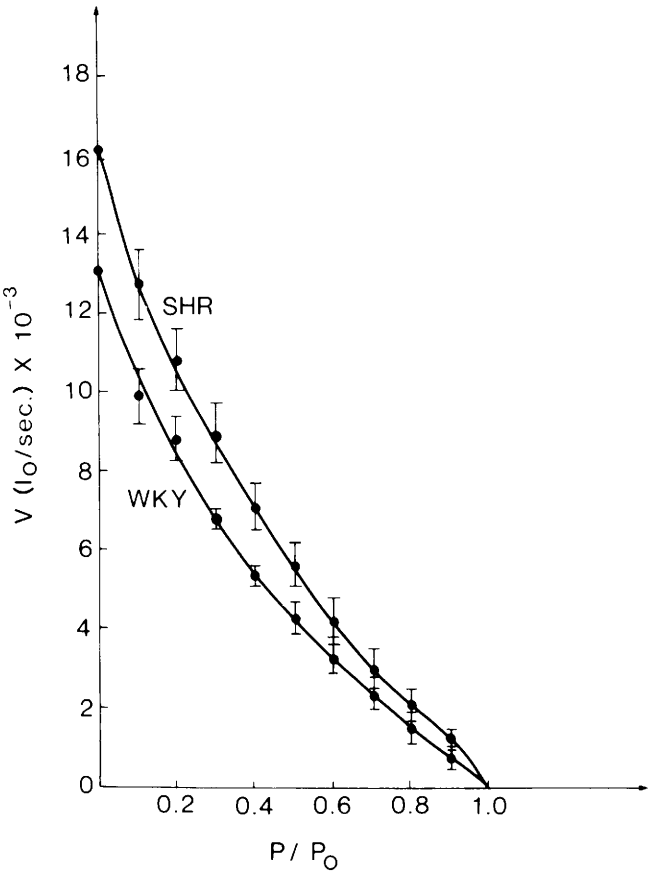

Figure 14. An illustration of the mean SHR (n = 6) and mean WKY (n = 5) caudal arterial muscle F-V curves from 16- to 18-week-old rats. The SHR curve is shifted above the WKY curve for all loads less than 80% P_o. Reprinted from Ref. 75, with permission from the National Research Council of Canada.

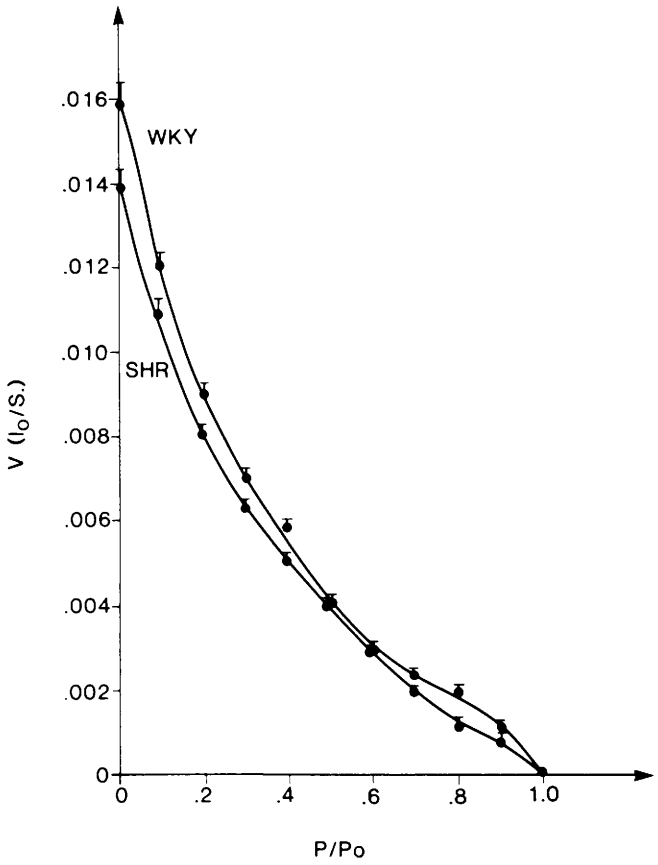

Figure 15. A comparison of the mean SHR (n = 7) and the mean WKY (n = 5) F-V curves from 28- to 31-week-old rats. The curves are almost superimposable on one another suggesting that velocity of shortening (cross-bridge cycling rate) decreases from once elevated velocities in hypertensive arterial muscle with chronic exposure to elevated transmural pressures and/or with hypertrophy.

terial muscle became necessary. Classical F-V curves (i.e., those made at times early in the shortening phase of contraction, but with varying load) cannot distinguish between the shortening velocities of the rapid-cycling and of the slow-cycling phases. Studying the velocity of shortening as a function of contraction time rather than as a function of the load on the muscle provides information regarding the mechanical behavior of these two different cycles.

A difference in the kinetics of either cycle in hypertensive compared with control muscle should be reflected in the dynamic stiffness. The dynamic stiffness is the inherent stiffness of the contractile apparatus (cross-bridge attachments) in actively contracting and/or relaxing muscle. Altered dynamic stiffness could be due to a difference in cross-bridge number or to a difference in cross-bridge cycling rate (i.e., a change in "on" time).

In one series of experiments, caudal arterial muscle strips were mounted vertically in a bath containing Krebs-Henseleit solution at 37°C and a 95% O_2/5% CO_2 gas mixture was bubbled through the bath. The lower end of the muscle strip was held rigidly while the upper end was tied to an electromagnetic lever system. The current through the coil of the electromagnet determined the load on the muscle. A detailed account of the apparatus and the response characteristics to abrupt alteration in load have previously been published (100, 101). The methodological and physiological aspects of studying abrupt alterations of load (the load-clamp technique) have also been reported (100, 102). The muscle strip was equilibrated for 2 hr prior to commencing the experiment. During the equilibration period, the muscle was stimulated isometrically every 5 min. Determination of the achievement of steady state was made by monitoring the maximum tetanic tension developed, rate of tension development, and contraction time for each consecutive contraction. Supramaximal electrical stimulation was via 17 V, 60 Hz AC for 7 sec through two platinum electrodes placed longitudinally on either side of the muscle strip in the bath. Following equilibration, optimal length for maximum tension development (l_o) was determined for each preparation by doing an active length-tension analysis. Contractions were always tetanic and instantaneous length, force, and velocity of shortening were recorded simultaneously and displayed as functions of

time by an HP 9836 microcomputer. Permanent records were produced on an HP 7470 A plotter. To eliminate the effect of load, the technique of zero load-clamping described by Brutsaert *et al.* (38) was employed. In this technique, the load on the muscle was abruptly (within 3 msec) clamped to zero. Two transients were seen as the load dropped from preload to zero. A fast shortening transient was seen immediately following the zero load clamp, which represented recoil of the muscle's series elastic component. This was followed by an artifactual oscillation and then a prolonged slow shortening. The maximum slope of the slow transient (V_0) represented the true average cycling activity of the cross-bridges. V_0 values were obtained at 0.5-sec intervals. The values were then plotted against time (t). Maximum V_0 was attained early in contraction and thereafter progressively declined.

Mean SHR and WKY V_0 (l_0/sec) versus t (sec) curves are compared in Figure 16. The mean SHR curve is significantly elevated above the mean WKY curve at all times after 3.0 sec until the end of the shortening phase of contraction, indicating that the SHR arterial muscle was faster than the WKY arterial muscle after 3.0 sec into contraction ($P < 0.01$). Prior to 3.0 sec, the SHR and WKY mean curves are superimposable, indicating that the SHR and WKY arterial muscle shortening velocities were the same from the onset of shortening until the maximum velocity of shortening was attained ($P > 0.05$). The data in Figure 16 also show that the SHR muscle was not only faster than the WKY muscle from 3.0 sec until the end of shortening, but was able to shorten for a longer period

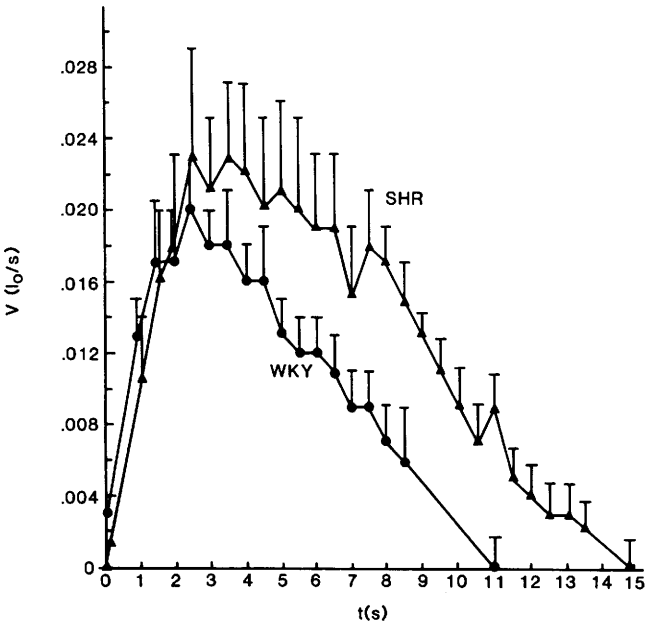

Figure 16. Comparison of the mean SHR (n = 7) and the mean WKY (n = 8) caudal arterial smooth muscle V (l_0/sec) versus t (sec) curves. The SHR curve is shifted above the WKY curve at all times later than 3.0 sec into contraction.

of the total contraction time. It can be seen that the SHR curve is not complete until 15.0 sec, while the WKY muscle returned to zero velocity at 11.0 sec.

In another series of experiments, in collaboration with Richard A. Meiss, caudal arterial strips were mounted horizontally in a muscle bath through which Krebs-Henseleit bubbled with a gas mixture 95% O_2/5% CO_2 and maintained at 37°C was circulated. One end of the arterial strip was attached to a stainless steel lever (Cambridge Instruments 300 H Dual Mode Servo). The other end of the strip was attached to a photoelectric force transducer. The apparatus has been described in detail previously (103). The arterial rings were equilibrated for 1 hr on the average prior to commencing the experiments. Stimulus-response data were obtained and the parameters of supramaximal electrical stimulation for the tissue were identified as 35 V, 60 Hz, 7 sec. Optimal length for tension development (l_0) was determined for each preparation by doing a limited length-tension analysis prior to commencing actual data collection. Muscle length and weight were obtained and cross-sectional area (CSA) was calculated for each preparation. During the experiments, afterloads and load-clamps were applied in random order with each consecutive contraction. Length and force were recorded simultaneously as functions of time (t) on a chart recorder (Gould, Brush 260). The dynamic stiffness of the caudal arterial preparations was measured throughout the contraction/relaxation cycle. In order to provide a continuous assessment, the method of sinusoidal oscillatory length perturbations (103–105) was used. This method involves applying small sinusoidal length perturbations (amplitude <0.2% of the muscle length, frequency 30 to 80 Hz) to the contracting muscle and measuring the amplitude of the resulting force perturbation. The dynamic stiffness is then computed as the ratio of the two amplitudes and is generally proportional to the force developed by the muscle. The increase in stiffness associated with active tension development was compared for hypertensive and normal arteries. That is to say, the slope of the normalized force/stiffness relationship was compared. In addition, SHR and WKY stress/strain versus force (N/cm^2) and stress/strain versus shortening (% l_0) curves were compared for isometrically and preloaded isotonically contracting muscle, respectively.

The mean dynamic stiffness (dF/dL) versus force curves for isometrically contracting and relaxing caudal arterial muscle are compared in Figure 17 for SHR (Panel A) and WKY (Panel B) tissue. The dynamic stiffness of the rat caudal arterial muscle was similar at any given level of developed force regardless of whether the muscle was in the contractile or relaxation phase ($P > 0.05$). The mean dynamic stiffness versus force curves of SHR and WKY isometrically contract-

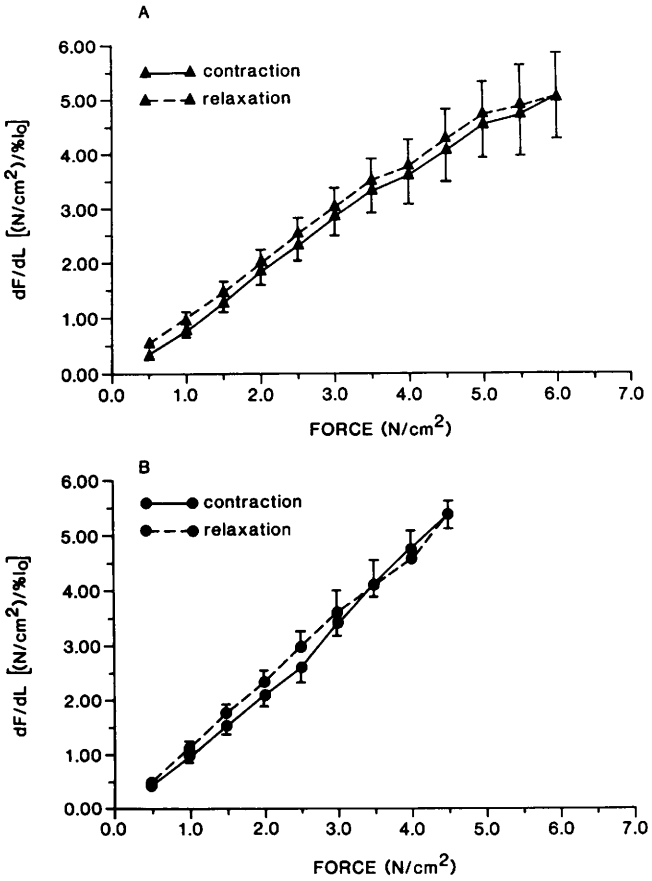

Figure 17. Panel A: A comparison of the mean dF/dL ([N/cm^2]/% l_o) versus force (N/cm^2) curves for isometrically contracting and relaxing SHR (n = 7) caudal arterial muscle. There is no significant difference between the curves, indicating that there is no difference in stiffness during relaxation compared with stiffness during contraction in this particular smooth muscle type. Panel B: A comparison of mean dF/dL ([N/cm^2]/% l_o) versus force (N/cm^2) curves for isometrically contracting and relaxing WKY (n = 6) caudal arterial muscle. As in Panel A, there is no significant difference between the curves, indicating no difference in stiffness during relaxation compared with that measured during contraction.

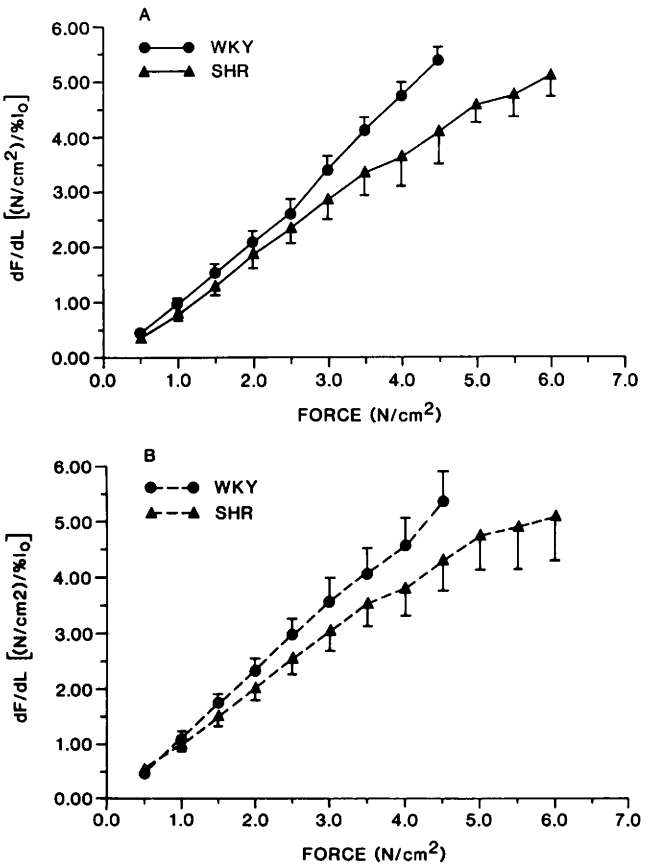

Figure 18. Panel A: A comparison of the mean SHR (n = 7) and WKY (n = 6) dF/dL ([N/cm^2]/% l_o) versus force (N/cm^2) curves for isometrically contracting caudal arterial muscle. Stiffness is significantly greater for the WKY muscle at the higher loads (>3.5 N/cm^2) than for SHR arterial muscle ($P < 0.05$). Panel B: A comparison of the mean SHR (n = 7) and mean WKY (n = 6) dF/dL ([N/cm^2]/% l_o) versus Force (N/cm^2) curves for isometrically relaxing caudal arterial muscle. Stiffness is significantly greater for the WKY muscle at onset of relaxation (i.e., at loads >4 N/cm^2) than for SHR arterial muscle ($P < 0.05$), but there is no difference in the stiffness once force has declined to <4 N/cm^2.

ing (Panel A) and relaxing (Panel B) are compared in Figure 18. At the higher loads (within 50% of P_o), the SHR muscle is less stiff than the WKY muscle during both contraction and relaxation when operating in isometric mode. The mean dF/dL versus shortening for isotonically contracting and relaxing caudal arterial muscle are compared in Figure 19 for SHR (Panel A) and WKY (Panel B) preparations. As was the case with the isometric dynamic stiffness, there is no difference in the stiffness at any given muscle length regardless of whether the muscle is shortening or relengthening ($P > 0.05$). The mean dynamic stiffness curves of SHR and WKY isotonically contracting (Panel A) and relaxing (Panel B) caudal arterial muscle are compared in Figure 20. The SHR muscle is significantly stiffer than the WKY muscle at all actively shortened lengths between resting length (l_o) and 2% l_o. There is no difference in the stiffness when the SHR and WKY muscle strips have shortened as much as or greater than 2% l_o.

Results of these experiments are consistent with the hypothesis that two functionally different cross-bridge states are operational during contraction in arterial muscle and, furthermore, show that this mechanism applies in both hypertensive (SHR) and normotensive (WKY) arterial muscle. There is currently much debate as to the biochemical regulation of smooth muscle cross-bridge rate. Possible candidates for alteration in the SHR muscle mechanics include myoplasmic calcium concentration (95) or changes in the intrinsic properties or amount of the various possible regulatory proteins such as caldesmon (106), calponin (107), or myosin light chain kinase or of the contractile protein, myosin.

There is some evidence based on stiffness measurements in canine tracheal muscle that the reduction in velocity later on in contraction is not due to a re-

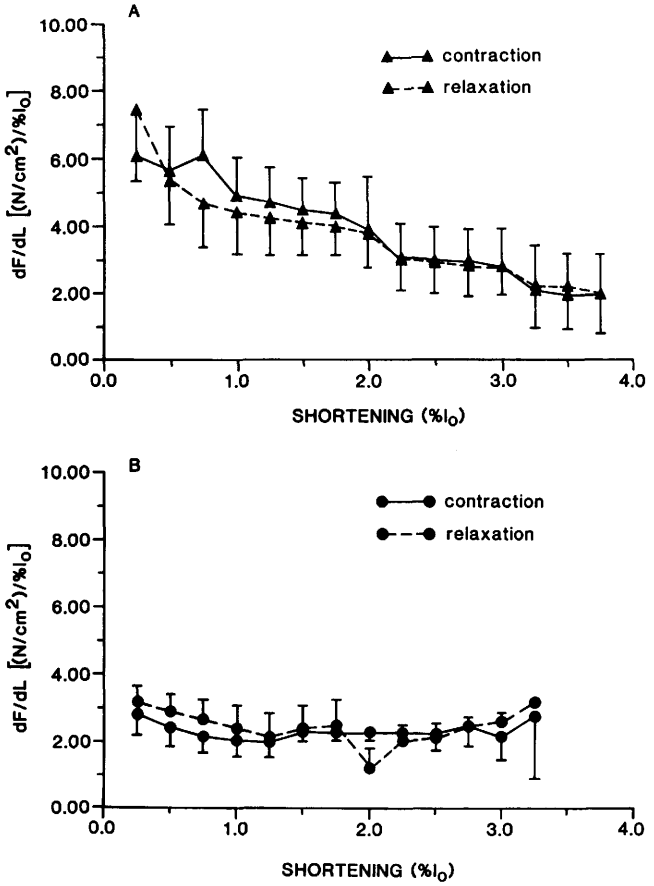

Figure 19. Panel A: A comparison of mean SHR (n = 7) dF/dL ([N/cm^2]/% l_o) versus shortening (% l_o) for preloaded isotonically contracting and relaxing (i.e., actively shortening and relengthening) caudal arterial muscle. Stiffness declines as the muscle shortens then increases again as the muscle lengthens. There is no difference in the stiffness of the muscle at the same particular length regardless of whether the muscle is in the shortening or relaxing phase. Panel B: A comparison of mean WKY (n = 6) dF/dL ([N/cm^2]/% l_o) versus shortening (% l_o) curves for preloaded isotonically contracting and relaxing (i.e., actively shortening and relengthening) caudal arterial muscle. Similarly to the SHR muscle, there is no difference in the stiffness of the WKY muscle at the same given length regardless of whether the muscle is in the shortening or relaxing phase. Unlike the SHR muscle, the WKY isotonic stiffness curve is relatively flat. There is no difference in stiffness throughout the contraction. The stiffness is the same for the WKY muscle whether it is maximally shortened or whether it is at its resting length.

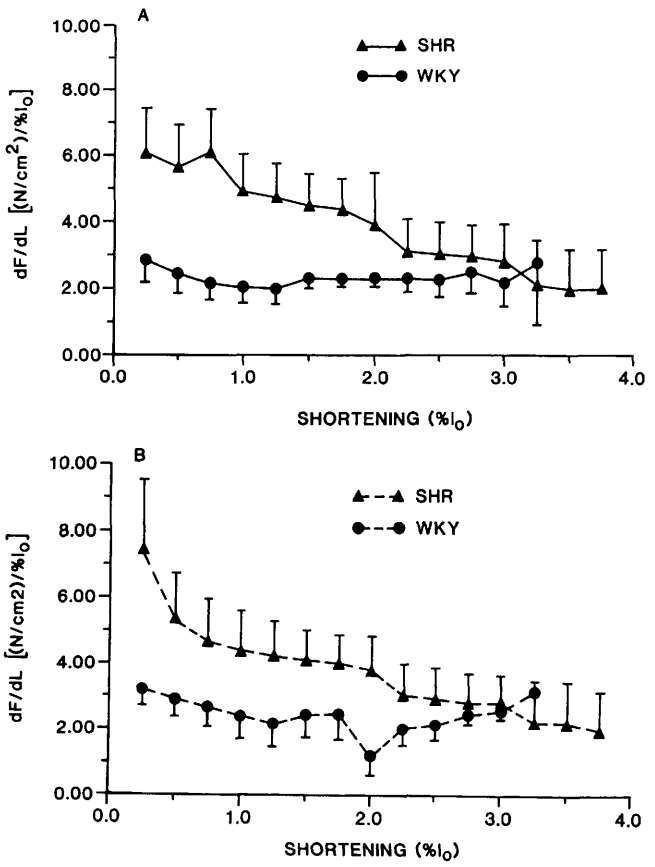

Figure 20. Panel A: A comparison of the mean dF/dL ([N/cm^2]/% l_o) versus shortening (% l_o) curves for isotonically contracting SHR (n = 7) and WKY (n = 6) caudal arterial muscle. The SHR curve is significantly elevated above the WKY curve from resting length until shortening of 2% l_o ($P < 0.05$) has occurred, indicating that the SHR muscle is twice as stiff as the WKY muscle at resting length and remains stiffer than the WKY muscle until it has shortened as much as, or greater than 2% l_o. Panel B: A comparison of the mean dF/dL ([N/cm^2]/% l_o) versus shortening (% l_o) curves for isotonically relaxing SHR (n = 7) and WKY (n = 6) caudal arterial muscle. There is no difference between the two curves at onset of relaxation (when the SHR muscle has shortened 3.5 to 4.0% l_o and the WKY muscle has shortened 3.0% l_o). However, the SHR curve is elevated above the WKY curve once sufficient lengthening has occurred, such that the muscle has relaxed to within 2.0% l_o ($P < 0.05$). The SHR muscle becomes increasingly stiffer than the WKY muscle as lengthening occurs during relaxation until resting length is achieved, at which point the SHR muscle is twice as stiff as the WKY muscle.

duction in the number of active cross-bridges (45). Therefore, the fall in velocity is likely due to mechanisms resulting in the transition of rapid-cycling to slow-cycling cross-bridges involving biochemical or conformational changes in existing bridges rather than recruitment of new bridges. It may be argued that there is an effect of muscle length on cross-bridge activity. However, velocity-length phase plane studies in canine tracheal muscle showed that velocity was length independent between 0.70 and 1.0 l_o, and since the average maximum shortening was 0.25 l_o, it was concluded that the progressive decrease in cycling rate was not due to length changes (45). This conclusion is even more obvious in the studies of arterial muscle cross-bridge cycling activity. WKY caudal arterial muscle has a maximum shortening of only about 6.5% l_o (75).

Two specific points on the V_o versus t curves (Fig. 16) stand out. The first is at the peaks of the curves. The peaks of the SHR and WKY mean curves occur at the same point in the time course of contraction (i.e., at 2.0 sec). However, the SHR velocity remains maximal until after 3.0 sec, while the WKY commences to decline immediately following 2.0 sec. The peak in these two curves likely indicates the point in time at which enough slow-cycling bridges have been recruited to result in an internal load great enough to significantly reduce velocity of shortening. The other

point of particular significance is the end point of the V_0 versus t curve. This point establishes the time in the course of an isotonic contraction at which further detectable shortening cannot occur even with negligible external load on the muscle. At this point in time, the internal resistance to shortening must be maximal, and the ratio of slow-cycling to rapid-cycling cross-bridges must be large. It is of particular interest physiologically that the SHR arterial muscle is able to produce active shortening for 15 sec, while the WKY muscle actively shortens for only 11 sec. This discrepancy means that the SHR arteries are capable of spending a greater proportion of each contraction, given the same degree of stimulation, in narrowing mode and this may account for some of the increased narrowing ability reported for SHR arteries (44, 75).

The dynamic stiffness of contracting and relaxing caudal arterial muscle was assessed by the method of applying small sinusoidal length perturbations to the maximally stimulated muscle strips. This method allows the continuous registration of muscle stiffness while having little effect on the muscle contractility. As in other muscle types investigated, the stiffness of isometrically contracting caudal arterial muscle increases with increasing contractile force in approximately linear fashion. However, the stiffness is not simply a function of muscle tension but depends also on the contractile state of the muscle. For instance, the stiffness of the normotensive WKY arterial muscle is greater during relaxation than during contraction at the same level of force developed. This is not the case for the hypertensive SHR muscle where stiffness parallels the rise and fall in force during both the contractile and relaxation phases (Table I). These results suggest that the contractile state of the hypertensive muscle is less changeable throughout the contraction than is the normotensive muscle. In other words, the numbers of cross-bridges rather than the cross-bridge state or kinetics may be the dominant contributor to dynamic stiffness in genetically hypertensive arterial muscle. The comparisons of the SHR with the WKY dynamic stiffness versus force curves and the V_0 versus time curves support this idea. As pointed out above, the velocity of shortening is less changeable over time for the hypertensive than for the normotensive muscle, indicating a predominance of the faster cross-bridge cycle. The fact that the SHR muscle is less stiff than the WKY muscle indicates that the hypertensive cross-bridges spend less "on" time during each cycle, at least later in the contraction or at the higher force levels. The hypertensive muscle appears to have a less pronounced "latch" phase than the normotensive muscle.

Table I. Ratios of the Slopes of the Isometric Relaxation Stress/Strain Curves Compared With Slopes of the Force Development Stress/Strain Curves

	SHR	WKY
	1.021	1.045
	0.995	1.059
	0.982	1.084
	1.022	1.015
	1.007	1.091
		1.040
Mean ± SEM	1.006 ± 0.008	1.056 ± 0.015[a]

[a] The mean ratio for the WKY group is significantly greater than the mean ratio for the SHR group ($P < 0.01$) and is also significantly greater than 1.0 ($P < 0.001$), while the mean ratio for the SHR group is not different from 1.0 ($P > 0.05$). These data indicate that the WKY caudal arterial muscle is stiffer during relaxation than it is during active force development.

The dynamic stiffness during isotonic contractions is independent of length changes and of time in the WKY muscle. Surprisingly though, the SHR arterial muscle stiffness is anomalously high within 2% of the resting length. The reason for the high stiffness at resting length that diminishes to normotensive levels during shortening in the hypertensive muscle is an enigma. Possibly some crossbridges ("latch" bridges) are attached, or remain made, in the SHR muscle during rest and then detach during shortening. This phenomenon might prove to be unique to the SHR arterial muscle rather than typical of normal smooth muscles as had been postulated by Butler *et al.* (49), as mentioned earlier. On the other hand, the very high stiffness at lengths approaching l_0 in isotonically contracting SHR arterial muscle may reflect differences in connective tissue elements and parallel elastic components.

Summary of the mechanical studies of arterial preparations from SHR, MK-421 trt SHR, and WKY rats allow the following conclusions: (i) the thickened arterial wall in the SHR appears to be secondary to the high blood pressure; (ii) SHR arterial muscle shortens more, shortens faster, and takes longer to relax than does WKY arterial muscle, while there is no difference in ability to develop tension; (iii) the latter is true of resistance arterial muscle as well as for larger muscular arterial muscle; and (iv) the faster shortening and slower relaxation rates of the SHR arterial muscle do not appear to be a result of high blood pressure and so may well be primary defects of arterial smooth muscle in these genetically hypertensive animals.

Arterial Wall Structure in Hypertension

A number of investigators have established that there is an increased wall-to-lumen ratio in blood vessels of hypertensives (28–34). This would indicate hypertrophy, hyperplasia, or both. Under conditions where the smooth muscle cells were fully relaxed, the internal radii of SHR brain and mesenteric arteries were smaller at all pressures compared with respect to

Table II. A Summary of Structural Changes of Mesenteric Arteries From SHR at Different Phases of Hypertension Development

	Vessel type	Prehypertensive	Developing	Established
Intima + IEL	SMA	—	—	?
	L	↑	↑	↑
	S	—	—	↑
Media	SMA	—	—	↑
	L	↑	↑	↑
	S	—[a]	↑	↑
Adventitia	SMA	—	—	↑
	L	↑	↑	↑
	S	—	↑	↑
Lumen	SMA	—	—	—
	L	—	—	—
	S	↓	—	—
SMC layers	SMA	—	—	—
	L	↑	↑	↑
	S	↑	↑	↑
Nerve density	SMA	—	—	?
	L	↑	—	?
	S	—	↑	?

Note. SMA = Superior mesenteric artery; L = large mesenteric artery; S = small mesenteric artery; — = no change; ↑ = increase; ↓ = decrease as compared with age-matched WKY; ? = not measured. Reproduced with permission from Ref. 31.
[a] Media to lumen ratio was significantly increased ($P = 0.005$).

the WKY (28). This encroachment of the thickened arterial wall on the arterial lumen would result in increased resistance and in elevated blood pressure. However, there is controversy as to whether these structural changes of the blood vessel wall are primary or secondary to the onset of high blood pressure, and little is known about the mechanism responsible for the thickened walls in hypertension.

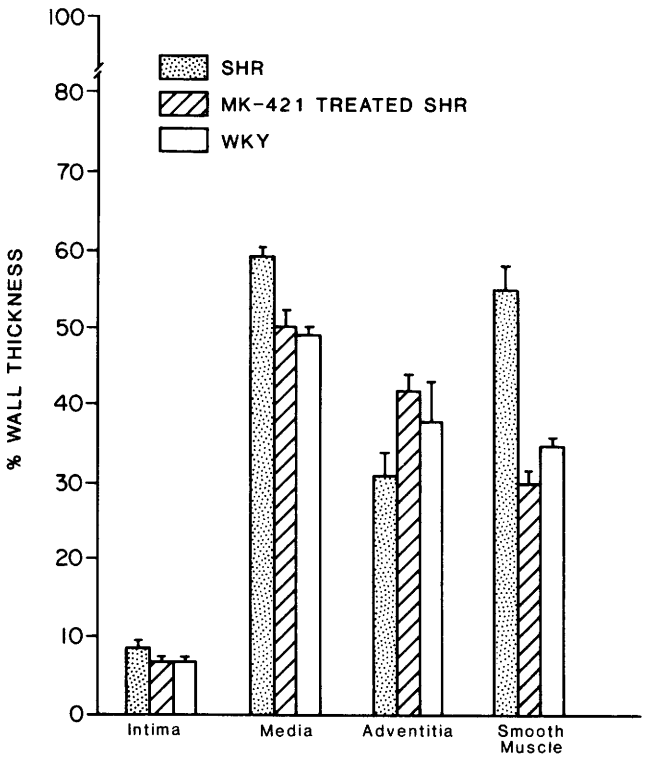

Figure 21. Histogram of the mean SHR, MK-421-treated SHR, and WKY mesenteric resistance arterial intima, media, adventitia, and smooth muscle thicknesses expressed as smooth muscle content.

Vascular muscle hypertrophy has been shown to be induced and/or increased by raised transmural pressures (92, 93). The cross-sectional area of smooth muscle cells in 5- to 6-month-old SHR vessels was reported to be 21% greater than that of cells in 5- to 6-month-old WKY vessels (88). Alterations of structural components which contribute to thickening of the vessel wall in SHR varies with the vessel type and also with the age of the animals (32). In particular, it was reported that 10- to 12-week SHR muscular arteries are composed of more smooth muscle cell layers compared with 10- to 12-week WKY muscular arteries. In

Table III. Structural Changes of Mesenteric Resistance Arteries in 18- to 21-Week-Old SHR Morphometrics (Mean ± SEM)

	SHR	MK-421-treated SHR	WKY
Intima	9.3 ± 1.2	7.3 ± 0.3	7.3 ± 0.3
(% wall)	(n = 3)	(n = 3)	(n = 3)
Media	59 ± 1[a]	50 ± 2	49 ± 1
(% wall)	(n = 3)	(n = 3)	(n = 3)
Adventitia	31 ± 3	42 ± 2	38 ± 5
(% wall)	(n = 3)	(n = 3)	(n = 3)
Smooth muscle	55 ± 3[a]	30 ± 2	35 ± 1
(% media)	(n = 3)	(n = 3)	(n = 3)
Wall/lumen	0.15 ± 0.02	0.10 ± 0.02	0.09 ± 0.01
(at 50 mm Hg)	(n = 4)	(n = 4)	(n = 3)
Smooth muscle	5.9 ± 0.2[a]	4.6 ± 0.4	4.2 ± 0.1
cell layers	(n = 5)	(n = 3)	(n = 3)

[a] A value that is significantly different ($P < 0.05$) from the other values in that row.

addition, volume densities of the smooth muscle cells in the media of these muscular arteries are found to be higher in the SHR (32). Twenty-eight-week-old SHR arterial media from muscular arteries showed no further increase in cell layers, but smooth muscle cell volume was greater and the media thicker than at 10–12 weeks (33). These same investigators found an increase in smooth muscle cell layers in smaller resistance arteries of both age groups of SHR. Similar findings for SHR mesenteric resistance arteries had been reported earlier (88). Brayden *et al.* (28) reported that the DNA content of mesenteric resistance arteries from 25-week-old SHR was elevated by nearly 30%. The amounts of actin and myosin when normalized to DNA content were unchanged in SHR compared with WKY. Neither the absolute amounts and concentrations (relative to tissue mass) of elastin nor of collagen were changed in the SHR vessels. These biochemical measurements are consistent with the results of morphometric studies reporting smooth muscle cell hyperplasia rather than hypertrophy in SHR resistance arterial walls (31, 108).

Hypertrophy of smooth muscle cells in muscular arteries, such as femoral or caudal arteries, of older (>8 weeks) SHR rats may be related to the effect of long duration of elevated blood pressure in these rats (33, 92, 93). However, there is some evidence that medial thickening in small mesenteric resistance arteries of SHR occurs prior to or in the absence of hypertension as shown in Table II (31). Yet, measurements of mesenteric resistance arterial wall thickness in MK-421 (enalapril maleate)-treated, and therefore normotensive, SHR as shown in Figure 21 and Table III do not agree with the results of Lee's study. The reasons for such discrepancies in the literature have yet to be made apparent.

Biochemistry of Smooth Muscle Contraction

The sliding filament theory has been developed primarily from detailed investigations of skeletal muscle, but the general organization of thick and thin filaments in smooth muscle is consistent with a similar mechanism of contraction (109, 110). However, the regulation of actin-myosin interactions in smooth muscle by calcium is more complex than in striated muscle, and several different biochemical mechanisms have been proposed. In thick filament regulation, Ca^{2+} binds to calmodulin (CM), and the Ca^{2+}-CM complex subsequently binds to and activates myosin light chain kinase (MLCK) (111). Activation of MLCK results in phosphorylation of the 20,000-dalton light chain subunit of myosin (MLC_{20}) and the stimulation of actin-activated Mg^{2+}-ATPase activity of smooth muscle myosin (112, 113). There is also evidence that phosphorylated smooth muscle myosin Mg^{2+}-ATPase activity may be further increased by Ca^{2+}, which may be related to Ca^{2+} binding directly to myosin (114–116). Ca^{2+} may also regulate actin-myosin interaction in smooth muscle via thin filament components. Ebashi (117) had proposed that Ca^{2+} activation is mediated by a thin filament protein complex referred to as leiotonin. Marston (118) has shown that isolated thin filaments which are capable of binding Ca^{2+} activate myosin Mg^{2+}-ATPase activity in a Ca^{2+}-dependent manner. Marston also reported that the phosphorylation of a 21,000-dalton protein component in thin filaments is associated with an increase in the quantity of high-affinity Ca^{2+}-binding sites on thin filaments and a decrease in the Ca^{2+} concentration required for half-maximal activation of actin-activated Mg^{2+}-ATPase activity. Thin filament preparations also contain, in addition to actin and tropomyosin, caldesmon (140 kDa) and calponin (32 kDa). Caldesmon can bind the calcium-calmodulin complex and can also be phosphorylated by endogenous kinases such as protein kinase C (105). Calponin was first described by Takahashi *et al.* (120) and has, like caldesmon, been shown to bind actin and calmodulin.

It is generally accepted that at least three, if not four, Ca^{2+} binding sites on CM are occupied for the activation of the various calmodulin-dependent enzymes (119). Activation associated with an increase in cytoplasmic Ca^{2+} concentration is the result of Ca^{2+} binding first to CM with subsequent binding of the Ca-CM complex to and activation of MLCK. Inactivation due to a decrease in cytoplasmic Ca^{2+} concentration follows a different pathway, however. The rate of inactivation is about three orders of magnitude faster when Ca^{2+} first dissociates from the $Ca^{2+}{}_4$-CM-MLCK complex. Phosphorylation of smooth muscle MLC_{20} by the $Ca^{2+}{}_4$-CM-MLCK complex is thought to allow the activation of myosin Mg^{2+}-ATPase by actin, whereas dephosphorylated myosin is not activated. Phosphoprotein phosphatases have been purified from smooth muscle (121, 122). The major role of phosphatases is to regulate the restoration of smooth muscle myosin to the nonphosphorylated form. Adelstein and Eisenberg (112) suggested that it is possible that one or both of the phosphatases purified from smooth muscle (phosphatase I and phosphatase II) (121) are always active in the resting cell. A rise in Ca^{2+}, which initiates contraction, might superimpose a dominant myosin kinase activity, whereas a decrease in Ca^{2+} would restore phosphatase activity to dominance.

A general scheme for the biochemical regulation of myosin phosphorylation in smooth muscle is represented in Figure 22. During the initiation of contraction, the concentration of intracellular free Ca^{2+} increases through influx across the sarcolemma and/or through the release of Ca^{2+} from intracellular stores. This results in an increase in Ca^{2+}-CM which then

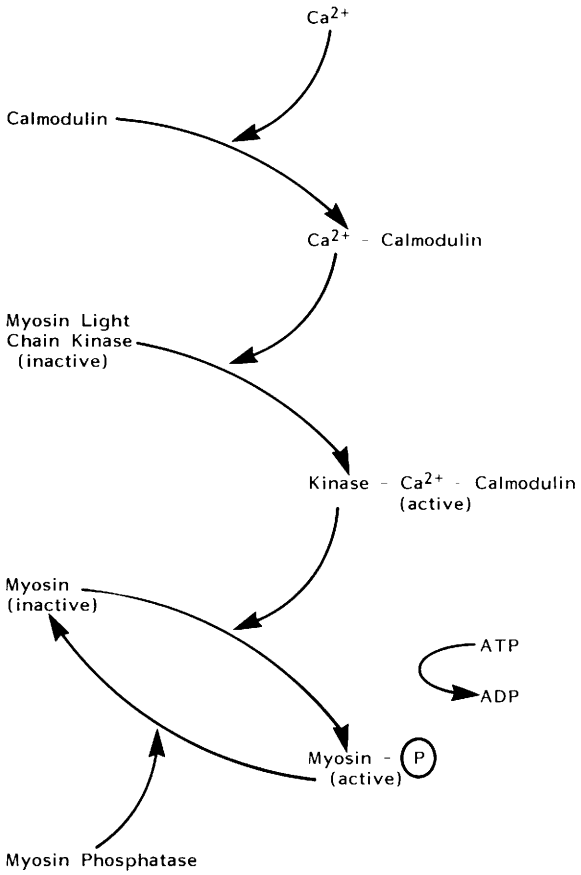

Figure 22. The cascade of intracellular reactions by which the contraction of smooth muscle is activated in the presence of Ca^{2+}. Myosin light chain kinase is the enzyme that catalyzes the phosphorylation of a particular site on the 20-kDa regulatory myosin light chain.

activates MLCK which phosphorylates MLC_{20} which results in an increase in myosin actin-activated Mg^{2+}-ATPase activity. Relaxation is caused by the sequestration and removal of Ca^{2+} from the sarcoplasm which results in the inactivation of MLCK by dissociating Ca^{2+} from the holoenzyme complex. Dephosphorylation of MLC_{20} by myosin phosphatase then inactivates myosin Mg^{2+}-ATPase.

In the sliding filament theory, developed force is attributed to the number of active cross-bridges generating force additively, this number being regulated by the binding of Ca^{2+} to specific regulatory proteins. Maximum shortening velocity (V_{max}) is interpreted as a direct reflection of cross-bridge cycling rate and could be determined by the isoenzymatic form of myosin in the cell. The hypothesis that MLC_{20} phosphorylation plays a direct role in determination of isometric force by activating a certain number of cross-bridges has been complicated by the observation that phosphorylation can decline in time while force is maintained (123). The transient increase and decrease in myosin phosphorylation indicates that phosphorylation of myosin may not be the sole Ca^{2+}-dependent regulatory event in smooth muscle contraction. It has been hypothesized that the transient increase in myosin phosphorylation is explained by a transient rise in cell Ca^{2+} concentration and that a second regulatory site responsible for Ca^{2+}-dependent force maintenance, necessarily has a greater Ca^{2+} sensitivity than the activation of MLCK by $Ca^{2+}{}_4$-CM (124).

Dillon and coworkers (47) discovered that, in parallel with phosphorylation, isotonic shortening velocity against light loads increases during the early phase of contraction and then declines while force rises to a maintained maximum in arterial muscle. Levels of myosin phosphorylation during maintained contractions correlate directly with V_{max} and not necessarily with absolute levels of stress (125). These observations have led to the hypothesis that the Ca^{2+}-dependent phosphorylation of myosin initiates rapid cycling of cross-bridges resulting in the development of isometric force and that, in the presence of a cytoplasmic Ca^{2+} concentration sufficient to maintain force, the dephosphorylation of myosin results in an attached non- or very slow cycling crossbridge (latch bridge). However, V_{max} has been observed to be dependent on Ca^{2+} and CM concentrations in permeabilized or "skinned" preparations (125, 126), and on extracellular Ca^{2+} concentration in intact smooth muscle preparations while the level of myosin phosphorylation remained constant (124). The decline in cross-bridge cycling rates during stimulation is reflected in measurements of energy consumption in contracting smooth muscle (49, 128, 129). The physiological importance of the hypothetical "latch" state is the provision of a mechanism whereby tonic force can be maintained more efficiently by reducing the ATP consumption associated with high cross-bridge cycling rates.

Contractile Protein Changes in Hypertensive Arterial Muscle

As discussed previously, SHR muscle displays increased shortening ability and increased shortening velocity, and that the increased velocity of shortening appears to be a primary alteration in the SHR muscle. Velocity of shortening is dependent on actomyosin ATPase activity, and this activity is, in turn, calcium dependent. Purified smooth muscle actomyosin, unlike that of skeletal muscle, has a low ATPase activity (95), and this increases as a result of phosphorylation of the 20-kDa regulatory myosin light chain (84). The enzyme catalyzing this phosphorylation, myosin light chain kinase (MLCK), requires both Ca^{2+} and calmodulin for activity. Numerous studies from different laboratories have demonstrated that a direct relationship exists between actin-activating myosin ATPase activity and the degree of phosphorylation of the 20-kDa myosin light chain (MLC_{20}) of smooth muscle (84,

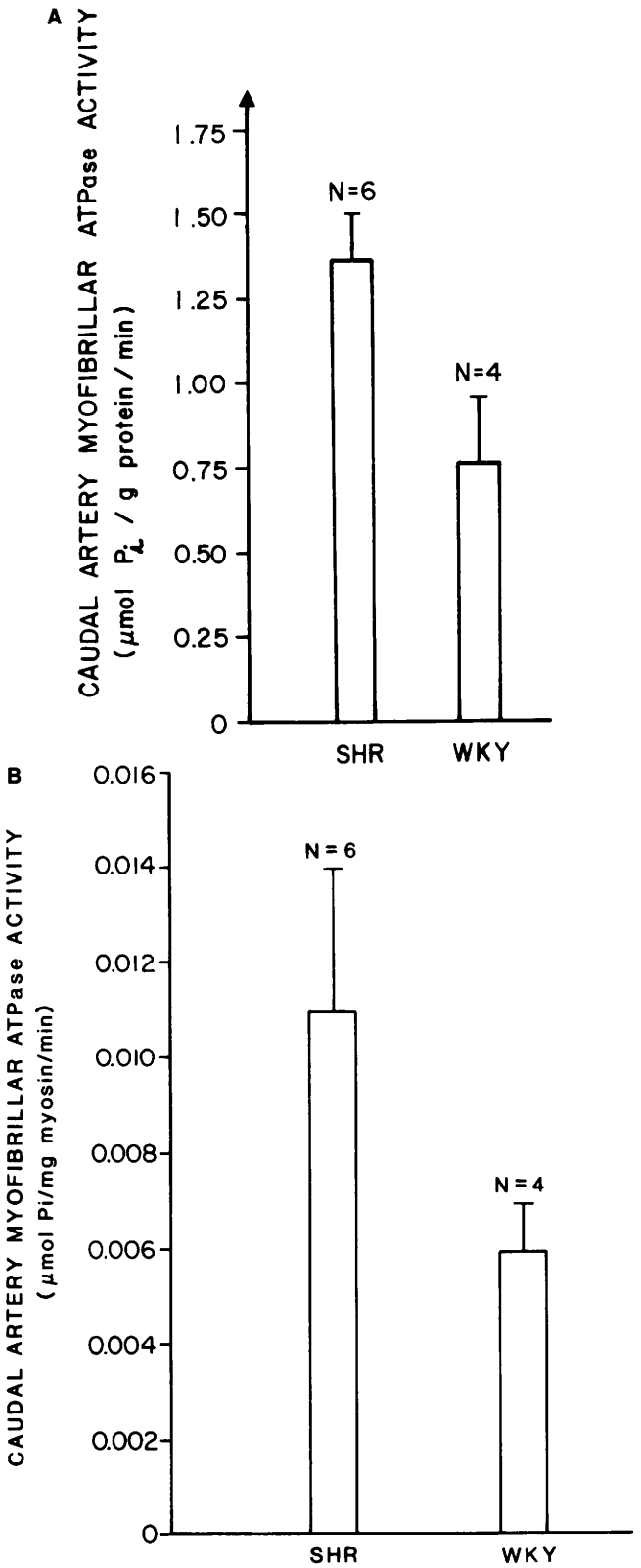

Figure 23. Histograms of the mean ± SE myofibrillar ATPase activities are normalized for myofibrillar protein weight (Panel A) and for myosin content (Panel B) of SHR and WKY caudal arterial smooth muscle. The SHR myofibrillar ATPase activity is significantly greater than the WKY myofibrillar ATPase activity regardless of the method of normalization. Adapted from Figures 1 and 2 of Ref. 69, with permission courtesy of the copyright holder Wiley-Liss, New York, NY, a division of John Wiley and Sons, Inc.

124, 125, 130–133). According to these investigators, it is surmised that the smooth muscle contractile system is regulated by phosphorylation and dephosphorylation of the MLC_{20} by the action of MLCK and phosphatase, respectively, depending on the presence or absence of calcium. On the other hand, with prolonged contraction times, maximum levels of isometric force can be maintained by vascular smooth muscle despite relatively low stoichiometry of myosin light chain phosphorylation (47). Nevertheless, the maximum velocity of shortening (V_{max}) is dependent on the actomyosin ATPase activity, and shortening ability is, at least to some extent, dependent on the velocity of shortening.

The existence of smooth muscle myofibrils has been reported in both smooth muscle tissue and cultured smooth muscle cells (134, 135). Sobieszek and Bremel (136) showed that the smooth muscle myofibrillar ATPase activity is much higher than that of actomyosin ATPase. They ascribed this difference to a loss of calcium sensitive ATPase activity in the latter during preparation since addition of myosin light chain kinase (MLCK) and calmodulin to the actomyosin could restore ATPase activity. Therefore, it is likely that myofibrillar ATPase activity, rather than the ATPase activity of a more purified system, quantitatively resembles more closely that of intact smooth muscle. Interestingly, SHR caudal arterial myofibrillar ATPase activity was found to be 1.8 times greater than the WKY caudal arterial myofibrillar ATPase activity for animals 16–18 weeks of age (Fig. 23A) (i.e., at the same stage of hypertension at which V_{max} was shown to be elevated). Furthermore, the difference in ATPase activity remained apparent when the data was normalized for myosin content as shown in Figure 23B ($P < 0.005$). Therefore, the difference in ATPase activity cannot be explained by an increase in actomyosin content which is known to occur in hypertrophied vascular muscle from SHR (28).

Altered actomyosin ATPase activity in hypertensive smooth muscle may be due to changes in the intrinsic properties of the enzyme such as a shift in myosin isoform or to an increased calcium concentration as it has been shown for smooth muscle that calcium concentration affects ATPase activity (95), or to changes in the type or amount of myosin light chain kinase. That isoenzymes exist in cardiac and skeletal muscle (63–65) is well established, and it has been reported that different myosin isoenzymes exist in smooth muscle (66, 69, 90). Furthermore, Sparrow *et al.* (66) have reported the existence of at least two different heavy chains of myosin in several different smooth muscle tissues and Gaylinn *et al.* (137) have reported two isoforms of the 20-kDa regulatory light chain in vascular smooth muscle. Three isoforms (a non-muscle isoform of 196–198 kDa and the 200- and

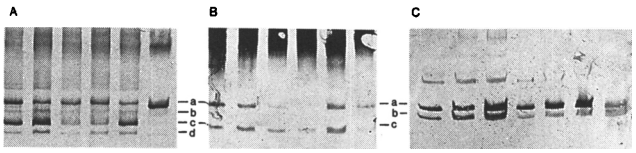

Figure 24. Photograph of typical western blots of SHR and WKY rat caudal arterial muscle MLC_{20}. Panel A: MLC_{20} from resting (Lanes 1 and 2) or electrically stimulated (6–7 sec; Lanes 2, 4, and 5) arterial and resting uterine (Lane 6) muscle treated with an isoform nonspecific MLC_{20} antibody. Bands a and b are nonphosphorylated and phosphorylated forms of the smooth muscle (SM) isoform of MLC_{20}, respectively. Bands c and d are the nonphosphorylated and phosphorylated forms of the nonmuscle (NM) isoform of MLC_{20}, respectively. The vascular muscle has significant amounts of both isoforms, while the uterine muscle apparently contains predominantly SM MLC_{20}. Panel B: MLC_{20} from EGTA in zero Ca^{2+}-treated (Lanes 1 and 3) or high K^+ (80 m*M*)-stimulated (>5 min; Lanes 2, 4, 5, and 6) arterial muscle treated with an isoform nonspecific MLC_{20} antibody. Only Band a and c, the nonphosphorylated forms of the smooth muscle and non-muscle isoforms, respectively, are apparent. Panel C: MLC_{20} from canine tracheal (Lanes 1–3), rat GI (Lanes 4–6) and rat caudal arterial (Lane 7) muscle under resting conditions in normal Ca^{2+} solution treated with a smooth muscle isoform specific MLC_{20} antibody. In this case, only Bands a and b, the nonphosphorylated and phosphorylated forms, respectively, of the SM MLC_{20} are apparent. The blots represented in Panel A and B of this photograph were produced with an isoform nonspecific antibody raised to bovine tracheal muscle MLC_{20} (gift of Dr. James T. Stull), while the blot in Panel C was produced with a smooth muscle isoform specific antibody raised to chicken gizzard muscle MLC_{20} (gift of Dr. David R. Hathaway).

204-kDa muscle isoforms) of the myosin heavy chain and two isoforms of the 20-kDa myosin light chain have been identified in SHR and WKY rat caudal arterial muscle. Table IV compares the mean ± SEM SHR (n = 16) caudal arterial muscle total myosin concentration, muscle myosin concentration, non-muscle myosin/muscle myosin ratio and the MHC_{200}/MHC_{204} ratio. The total myosin concentration is increased in SHR muscle ($P < 0.001$) in agreement with the previous studies by Brayden *et al.* (28). Similarly, the muscle myosin concentration is increased in the SHR muscle ($P < 0.001$). The SHR and WKY non-muscle myosin/muscle myosin ratios are not different ($P > 0.001$), nor are the SHR and WKY MHC_{200}/MHC_{204} ratios different ($P > 0.05$). Therefore, while the total myosin concentration increases as the arterial muscle hypertrophies, the relative proportion of MHC isoform remains constant. These results are perhaps not surprising given that most reports of similar studies do not show a correlation between shifts in MHC isoform ratios and changes in parameters of contractility. There are a few exceptions (71, 72), but one wonders if a positive correlation is merely a coincidence and whether MHC isoforms have any affect on shortening velocity in smooth muscle at all. The latter remains to be elucidated. Shifts in MHC isoforms may prove to be more important in mechanisms of smooth muscle proliferation (91) and phenotypic change (90).

Figure 24 shows a photograph of Western blots of MLC_{20} from a variety of smooth muscles. The smooth muscle (SM) MLC_{20} isoform was identified in a series of experiments on a variety of smooth muscle types (Panel C) as the two upper bands (a and b—nonphosphorylated and phosphorylated, respectively) with the use of a SM MLC_{20}-specific antibody raised to chicken gizzard MLC_{20} (gift of Dr. David Hathaway). The majority of SHR and WKY caudal arterial MLC_{20} experiments were carried out with a MLC_{20} isoform nonspecific (but high-affinity) antibody raised to bovine tracheal muscle MLC_{20} (gift of Dr. James Stull) and resulted in blots with four bands (a, b, c, and d) of MLC_{20} like the one shown in Figure 24A. When neither isoform was phosphorylated to any significant extent as when the muscle was treated with EGTA in a zero Ca^{2+} solution or when the muscle was fast-frozen after several minutes (>5 min) into the plateau of force development in response to 80 m*M* K^+ stimulation, then only Bands a and c were evident as shown in Figure 24B. Table V presents the results of the SHR and WKY caudal arterial muscle MLC_{20} experiments. Both the SHR and WKY caudal arterial muscle contains almost equal amounts of the smooth muscle isoform (SM MLC_{20}) and the non-muscle isoform (NM MLC_{20}) of the light chain ($P > 0.05$). The mean SHR caudal arterial muscle phosphorylated SM MLC_{20}/nonphosphorylated SM MLC_{20} ratio is significantly greater than the mean WKY ratio in response to maximum electrical stimulation for a duration of 6–7 sec ($P < 0.05$). Interestingly, there is no difference in the SHR and WKY phosphorylated NM-MLC_{20}/nonphosphorylated NM-MLC_{20} ($P > 0.05$). These data suggest that the smooth muscle and non-muscle isoforms of MLC_{20} may be independently phosphorylated (i.e., may be independently regulated). Although a recent report by Monical *et al.* (138) contradicts this

Table IV. Myosin Concentration and MHC Isoform Ratios in SHR and WKY Caudal Arterial Muscle (Mean ± SEM)

	Total (myosin) (μg/500 μg tissue)	Muscle (myosin) (μg/500 μg tissue)	Non-muscle myosin/ muscle myosin	MHC_{200}/MHC_{204}
SHR (n = 16)	6.99 ± 0.30[a]	5.96 ± 0.20[a]	0.178 ± 0.003	0.546 ± 0.023
WKY (n = 16)	4.66 ± 0.20	4.04 ± 0.16	0.158 ± 0.006	0.464 ± 0.016

Note. Reprinted from Ref. 69 with permission from Wiley-Liss, New York, NY, a division of John Wiley and Sons, Inc.
[a] $p < 0.001$.

finding. At any rate, given that an increase in SM-MLC_{20} phosphorylation levels can explain the increased myofibrillar ATPase activity in SHR arterial muscle, the next question is: what is the cause of the increased MLC_{20} phosphorylation?

While myofibrillar protein may be the better preparation for estimating intact smooth muscle actomyosin ATPase activity as discussed earlier, it must be remembered that a myofibrillar preparation contains proteins other than actin and myosin and therefore complicates mechanistic speculation. One contaminant likely to affect the ATPase activity is caldesmon. Caldesmon is known to be an inhibitor of actomyosin ATPase. Caldesmon is a major actin-binding protein in smooth muscle, binding one caldesmon per seven actin at saturation. Caldesmon also binds the calcium-calmodulin complex and can be phosphorylated by endogenous protein kinases, such as protein kinase C. When calmodulin is bound to caldesmon, binding affinity for actin is decreased (106). Therefore, it cannot be ruled out that the SHR myofibrillar protein increased ATPase activity may be due to lower caldesmon concentration in SHR vascular smooth muscle. Another possibility is an altered calponin concentration in SHR vascular muscle. Calponin may be the smooth muscle equivalent of the Ca^{2+}-binding, actin-binding skeletal muscle protein troponin (107).

There are several other possibilities to explain an elevated level of actomyosin ATPase activity in hypertensive smooth muscle. One possible explanation may be an increased calcium concentration in hypertensive smooth muscle as it has been shown for smooth muscle that an increased calcium concentration causes an increased ATPase activity (95). One might envision that Aoki's "Calcium Membrane Theory of Essential Hypertension" (22) is quite correct and that the initial genetic defect in the arterial muscle is in the Ca^{2+} ATPases or channel proteins of the sarcolemma and/or SR. The data reviewed in the current manuscript would then provide the proof of the rest of the story (i.e., the intracellular mechanisms that are altered subsequent to the defect in Ca^{2+} handling and that actually result in the increased arterial muscle contractile activity and increased vascular resistance). The "Calcium Membrane Theory" and the data and ideas of this review might be incorporated into one concise theory: "The Hypercontractile Arterial Muscle Theory of Essential Hypertension." Another explanation for increased actomyosin ATPase activity may be changes in type or amount of MLCK. Calcium concentrations in the solutions were controlled and were the same in the SHR and WKY ATPase activity assays. However, it is still possible that there may be an increased calmodulin-bound calcium either due to increased calmodulin concentration in the SHR myofibrillar protein or more Ca^{2+} initially available for binding calmodulin prior to processing the tissue. These latter two possibilities seem most likely since the SHR smooth muscle MLC_{20} shows a 2.8 times higher phosphorylation level than the WKY SM MLC_{20} in response to supramaximal electrical stimulation. The velocity of smooth muscle shortening depends upon the level of MLC_{20} phosphorylation which depends upon the Ca^{2+} concentration, the Ca^{2+}-calmodulin concentration and the MLCK activity.

In Summary

Table VI compares the mean SHR caudal arterial maximum velocity of shortening (V_{max}), myofibrillar ATPase activity and SM MLC_{20} phosphorylation levels with the mean WKY V_{max}, myofibrillar ATPase activity and SM MLC_{20} phosphorylation levels, respectively. The SHR V_{max} is about 1.3 times greater than the WKY V_{max} (75). The SHR myofibrillar ATPase activity is about 1.8 times greater than the WKY myofibrillar ATPase activity (69). Lastly, the SHR phosphorylated SM MLC_{20}/nonphosphorylated SM MLC_{20} ratio is about 2.8 times greater than the WKY ratio. These and other results indicate the following: (i) while the caudal arterial muscle myosin concentration is increased by 47% in 16- to 18-week-old SHR (likely as a result of the hypertrophy and hyperplasia known to occur in SHR arterial muscle) (28), this increased myosin content is not responsible for the increased myofibrillar ATPase activity in the hypertensive muscle (69); (ii) the non-muscle myosin and the muscle myosin concentrations are increased proportionately in the SHR arterial muscle; (iii) there is no difference in the myosin heavy chain or MLC_{20} isoform pattern in the SHR compared with the WKY arterial muscle. Therefore, a difference in myosin isoform pattern does not occur with hypertrophy and/or hyperplasia of spontaneously hypertensive arterial smooth muscle (at least not at an early stage) and is not responsible for the increased V_{max} and increased shortening ability of hypertensive arterial smooth muscle. Furthermore, the conclusion that a shift in myosin heavy chain isoform is not a causative mechanism for spontaneous hypertension in the rat is supported by the work of Sparrow *et al.* (139). The shortening velocity, myofibrillar

Table V. MLC_{20} Isoforms and Phosphorylation in SHR and WKY Caudal Arterial Muscle (Mean ± SEM)

	NM MLC_{20}/ SM MLC_{20}	NM MLC_{20}-P/ NM MLC_{20}	SM MLC_{20}-P/ SM MLC_{20}
SHR (n = 10)	1.07 ± 0.44	0.42 ± 0.09	0.39 ± 0.07[a]
WKY (n = 6)	0.81 ± 0.26	0.44 ± 0.09	0.14 ± 0.09

[a] $P < 0.05$.

Table VI. Comparison of SHR and WKY Caudal Arterial Muscle V_{max}, Myofibrillar ATPase Activity and MLC_{20} Phosphorylation (Mean ± SEM)

	V_{max} (l_0/sec)	Myofibrillar ATPase activity (μm P_i/g protein/min)	SM MLC_{20}-P/ SM MLC_{20}
SHR	0.016 ± 0.001[a] (n = 6)	1.36 ± 0.13[a] (n = 6)	0.39 ± 0.07[a] (n = 10)
WKY	0.013 ± 0.001 (n = 5)	0.76 ± 0.19 (n = 4)	0.14 ± 0.09 (n = 6)

[a] $P < 0.05$.

ATPase activity, and MLC_{20} phosphorylation data all correlate and suggest that a difference in available free Ca^{2+} or in a regulatory protein, such as MLCK, is a plausible causative mechanism in genetic hypertension.

Finally, one wonders if any of the results of investigations of vascular smooth muscle from spontaneously hypertensive rats reviewed in this manuscript may hold true for vascular muscle from human essential hypertensives. While little information on human vascular muscle is available an intriguing tidbit of data acquired serendipitously by Dr. George Wyse (personal communication) is presented in Figure 25. Interestingly, in a study of human meso-appendix artery relaxation behavior, Wyse found that one preparation was considerably slower to relax than all the others. Upon examining the medical history of the individual from whom the slowly relaxing vessel was excised, it was discovered that the subject was a recently diagnosed, untreated essential hypertensive young man. While this may be a chance coincidental occurance only, one cannot help but wonder if indeed there is a cause-and-effect relationship. Certainly, careful investigation of human hypertensive vascular muscle function is warranted.

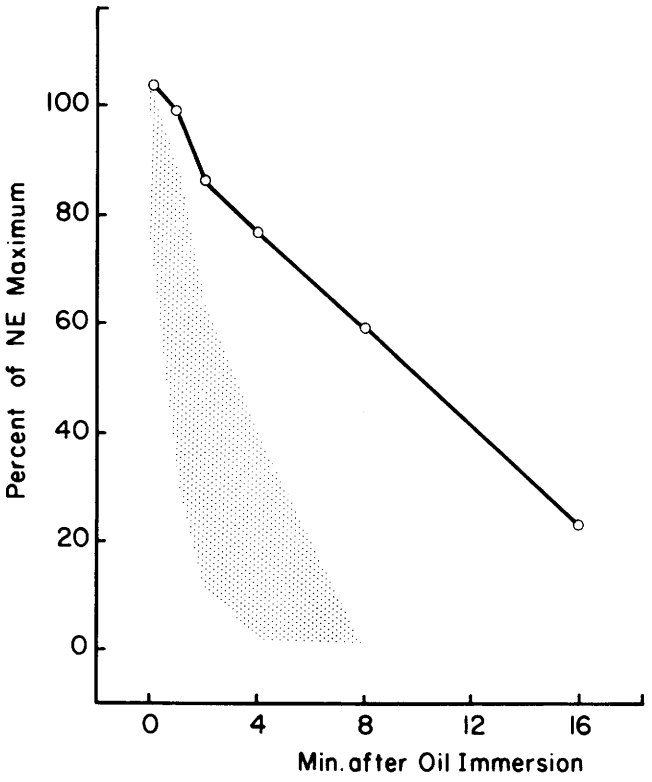

Figure 25. Relaxation phases of maximum isometric norepinephrine-stimulated contractile responses of isolated human meso-appendix arterial preparations. Relaxation phases are presented as the decline in force normalized as percent of each preparations maximum active force in response to NE as a function of time in minutes following oil immersion of each preparation. Oil immersion eliminates the effect of NE diffusion away from the preparation and possibly oxidation of NE (i.e., breakdown of the stimulus) on the relaxation rate. The majority of the data come from vessels from normotensive individuals (n = 10–12) and is presented as the mean and the confidence intervals of the mean values in the shaded area. The one outlier comes from an artery from a young hypertensive man. Courtesy of D. George Wyse, Professor and Head, Division of Cardiology, Foothills Hospital, University of Calgary, Calgary, Alberta, Canada.

The author is most grateful to the many colleagues who have offered helpful suggestions and good ideas, and have carried out countless difficult experiments both in the fields of vascular smooth muscle and systemic hypertension over the past two to three decades that have made this review article possible. Thanks are also due to the Canadian Heart Foundation and to the American Heart Association: Indiana Affiliate for supporting the hitherto unpublished studies presented in this review. Finally, special thanks to Dr. R. A. Meiss for assistance with the dynamic stiffness studies and to Dr. George Wyse for allowing the presentation and discussion of his data on human arterial relaxation and to Nancy Christian for expert typing of this manuscript.

1. Joint National Committee on Detection, Evaluation, and Treatment of High Blood Pressure. A cooperative study. JAMA **237**:255, 1977.
2. Kaplan NM. Essential hypertension. In: Clinical Hypertension (2nd ed). Baltimore, MD: Williams and Wilkins Co., pp44–93, 1978.
3. Page IH. Arterial hypertension in retrospect. Circ Res **34**:133–142, 1974.
4. Chien S. Blood rheology in hypertension and cardiovascular diseases. Cardiovasc Med **2**:356–360, 1977.
5. Letcher RL, Chien S, Pickering TG, Laragh JH. Elevated blood viscosity in patients with borderline essential hypertension. Hypertension **5**:757–762, 1983.
6. Shepherd JT, Vanhoutte PM. Hypertension and hyperreactivity of the cardiovascular system. In: Sheperd, JT and Vanhoutte, PM, Eds. The Human Cardiovascular System. New York: Raven Press, pp208–221, 1979.
7. Wright GL. The vascular sensitizing character of plasma from spontaneously hypertensive rats. Can J Physiol Pharmacol **59**:1111–1116, 1981.
8. Bricker NS. Natriuretic factors. Chairman's Address, IUPS XXXth. Congress, Vancouver, 1986.
9. Friedman SM, Butt RM, Friedman CL. Cation shifts and blood pressure regulation in the dog. Am J Physiol **190**:507–512, 1958.
10. Blaustein MP. Sodium ions, calcium ions, blood pressure regulation and hypertension: A reassessment and a hypothesis. Am J Physiol **232**:C165–C173, 1977.
11. Jones AW. Reactivity of ion fluxes in rat aorta during hypertension and circulatory control. Fed Proc **33**:133–137, 1974.
12. Haddy FJ. The role of a humoral Na-K pump inhibitor in experimental low renin hypertension. Symposium: The Role of Sodium in Hypertension. University of British Columbia, Vancouver, Canada, 1981.

13. Tobian L, Janacek J, Tomboulan A, Ferreira D. Sodium and potassium in the walls of arterioles in experimental and renal hypertension. J Clin Invest **40**:1922–1925, 1967.
14. Tobian L, Olson R, Chesley G. Water content of arteriolar wall in renovascular hypertension. Am J Physiol **216**:22–24, 1969.
15. Weinberger MH. Role of sympathetic nervous system activity in the blood pressure response to long-term captopril therapy in severely hypertensive patients. Am J Cardiol **49**:1542–1543, 1982.
16. Stekiel WJ, Contney SJ, Lombard JH. Effect of age on *in situ* small mesenteric veins (SmV) transmembrane potentials (Em) and their response to norepinephrine in spontaneously hypertensive rats (SHR). Fed Proc **41**:1094, 1982.
17. Postnov YV, Orlov SN. Ion transport across plasma membrane in primary hypertension. Physiological Rev **65**:904–945, 1988.
18. Kwan CY, Belbeck L, Daniel EE. Abnormal biochemistry of vascular smooth muscle plasma membrane as an important factor in the initiation and maintenance of hypertension in rats. Blood Vessels **16**:259–268, 1979.
19. Kwan CY. Abnormalities of vascular muscle membranes in hypertension with special reference to calcium handling. In: Kwan CY, Ed. Membrane Abnormalities in Hypertension. Boca Raton, FL: CRC Press, pp115–143, 1989.
20. Erne P, Bolli P, Bürgisser E, Bühler F. Correlation of platelet calcium with blood pressure. N Engl J Med **310**:1084–1088, 1984.
21. Erne P, Hermsmeyer K. Intracellular vascular muscle Ca^{2+} modulation in genetic hypertension. Hypertension **314**:145–151, 1989.
22. Aoki K. The calcium membrane theory of essential hypertension. In: Aoki K, Frohlich ED, Eds. Calcium in Essential Hypertension. San Diego, CA: Academic Press, pp623–655, 1989.
23. Rho JH, Newman B, Alexander N. Altered *in vitro* uptake of norepinephrine by cardiovascular tissues of spontaneously hypertensive rats. Hypertension **3**:704–709, 1983.
24. Webb RC, Vanhoutte PM. Sensitivity to noradrenaline in isolated tail arteries from spontaneously hypertensive rats. Clin Sci **57**:31s–33s, 1979.
25. Webb RC, Vanhoutte PM, Bohr DF. Inactivation of released norepinephrine in rat tail artery by neuronal uptake. J Cardiovasc Pharmacol **2**:121–132, 1980.
26. Patel KP, Kline RL, Mercer PF. Noradrenergic mechanisms in the brain and peripheral organs of normotensive and spontaneously hypertensive rats at various ages. Hypertension **3**:682–690, 1981.
27. Zsoter TT, Wolchinski C. Norepinephrine uptake in arteries of spontaneously hypertensive rats. Clin Invest Med **6**:191–195, 1983.
28. Brayden JE, Halpern W, Brann LR. Biochemical and mechanical properties of resistance arteries from normotensive and hypertensive rats. Hypertension (Dallas) **5**:17–25, 1983.
29. Mulvany MJ, Nilsson H, Nyborg N, Mikkelson E. Are isolated femoral resistance vessels or tail arteries good models for the hindquarter vasculature of spontaneously hypertensive rats? Acta Physiol Scand **116**:275–283, 1982.
30. Owens GK, Rabinovitch PS, Schwartz SM. Smooth muscle cell hypertrophy versus hyperplasia in hypertension. Proc Natl Acad Sci USA **78**:7759–7763, 1981.
31. Lee RMKW. Vascular changes at the prehypertensive phase in the mesenteric arteries from spontaneously hypertensive rats. Blood Vessels **22**:105–126, 1985.
32. Lee RMKW, Forest JB, Garfield RE, Daniel EE. Ultrastructural changes in mesenteric arteries from spontaneously hypertensive rats. Blood Vessels **20**:72–91, 1983.
33. Lee RMKW, Garfield RE, Forrest JB, Daniel EE. Morphometric study of structural changes in the mesenteric blood vessels of spontaneously hypertensive rats. Blood Vessels **20**:57–71, 1983.
34. Packer CS, Stephens NL. Tension-velocity relationships in hypertensive mesenteric resistance arteries. Can J Physiol Pharmacol **63**:675–680, 1985.
35. Johansson B. Vascular smooth muscle reactivity. Annu Rev Physiol **43**:359–370, 1981.
36. Shibata S, Cheng JB. Vascular relaxation in hypertensive rats. In: Valhoutte, PM and Leusen I, Eds. Mechanisms of Vasodilatation. Satellite Symposium to the International Congress of Physiological Sciences, Wilrijk, Belgium, 1978. Karger: Basal, pp181–186, 1977.
37. Zweifach BW, Kovalcheck S, DeLano F, Chen P. Micropressure-flow relationships in a skeletal muscle of spontaneously hypertensive rats. Hypertension (Dallas) **3**:601–604, 1981.
38. Brutsaert DL, Claes VA, Sonnenblick EH. Velocity of shortening of unloaded heart muscle and length-tension relation. Circ Res **19**:63–75, 1971.
39. Gordon AR, Siegman MJ. Mechanical properties of smooth muscle. I. Length-tension and force-velocity relations. Am J Physiol **221**:1243–1249, 1971.
40. Hill AV. The heat of shortening and the dynamic constants of muscle. Proc R Soc London B **126**:136–195, 1938.
41. Edman KAP, Mulieri LA, Scubon-Mulieri B. Nonhyperbolic force-velocity relationship in single muscle fibres. Acta Physiol Scand **98**:143–156, 1976.
42. Edman KAP. The force-velocity relation in striated muscle, its dependence on myosin isoform composition. In: Sellin LC, Libelius R, Thesleff S, Eds. Neuromuscular Junction, Proceedings of the Eric K. Fernstrom Symposium. New York: Elsevier, pp355–367, 1989.
43. Ross J, Covell JW, Sonnenblick EH, Taylor RR. Contractile state of the *in situ* heart. In: Tanz RD, Kavaler F, Roberts J, Eds. Factors Influencing Myocardial Contractility. New York: Academic Press, pp189–197, 1967.
44. Packer CS, Stephens NL. Mechanics of caudal artery relaxation in control and hypertensive rats. Can J Physiol Pharmacol **63**:669–674, 1985.
45. Stephens NL, Kagan ML, Packer CS. Time dependence of shortening velocity in tracheal smooth muscle. Am J Physiol **251**(Cell Physiol 20):C435–C442, 1986.
46. Packer CS, Kagan ML, Kagan JF, Robertson SA, Stephens NL. The effect of 2,3-butanedione monoxime (BDM) on smooth muscle mechanical properties. Pflügers Archiv **412**:659–664, 1988.
47. Dillon PF, Aksoy MO, Driska SP, Murphy RA. Myosin phosphorylation and the cross-bridge cycle in arterial smooth muscle. Science (Washington, DC) **211**:495–497, 1981.
48. Hai C, Murphy RA. Cross-bridge phosphorylation and regulation of latch state in smooth muscle. Am J Physiol **254**(Cell Physiol 23):C99–C106, 1988.
49. Butler TM, Siegman MJ, Mooers SU. Chemical energy usage during shortening and work production in mammalian smooth muscle. Am J Physiol **244**:C234–C242, 1983.
50. Siegman MJ, Butler TM, Mooers SU, Davies RE. Chemical energetics of force development, force maintenance, and relaxation in mammalian smooth muscle. J Gen Physiol **76**:609–629, 1980.
51. Stephens NL, Skoog CM. Tracheal smooth muscle and rate of oxygen uptake. Am J Physiol **226**:1462–1467, 1974.
52. Huxley AF. Muscle structure and theories of contraction. Prog Biophys Biophys Chem **7**:255–318, 1957.
53. Stephens NL, Kroeger EA, Metha JA. Force-velocity characteristics of respiratory airway smooth muscle. J Appl Physiol **26**:685–692, 1969.
54. Herlihy JT, Murphy RA. Force-velocity and series elastic characteristics of smooth muscle from the hog carotid artery. Circ Res **34**:461–466, 1974.
55. Hellstrand P, Johansson B. The force-velocity relation in phasic contractions of various smooth muscles. Acta Physiol Scand **93**:157–166, 1975.
56. Berg S. Vesical contractility. I. The force-velocity relationship as an index of contractility. Invest Urol **9**:431–437, 1972.
57. Close RI. Dynamic properties of mammalian skeletal muscle. Physiol Rev **52**:129–197, 1972.
58. Sonnenblick EH. Instantaneous force-velocity determinants in the contraction of heart muscle. Circ Res **16**:441–451, 1965.
59. Dobrin PB. Mechanical properties of arteries. Physiol Rev **58**:397–460, 1978.

60. Barany M. ATPase activity of myosin correlated with speed of muscle shortening. J Gen Physiol **50**:197–218, 1967.
61. Ruegg JC. Smooth muscle tone. Physiol Rev **51**:201–248, 1971.
62. Murphy RA. Contractile system function in a mammalian smooth muscle. Blood Vessels **13**:1–23, 1976.
63. Hoh JF. Light chain distribution of chicken skeletal muscle myosin isoenzymes. FEBS Lett **90**:297–300, 1978.
64. Beckers-Bleukx G, Marechal G. Detection and distribution of myosin in vertebrate smooth muscle. Eur J Biochem **152**:207–211, 1985.
65. Litten III RZ, Martin BJ, Low RB, Alpert NR. Altered myosin isozyme patterns from pressure-overloaded and thyrotoxic hypertrophied rabbit hearts. Circ Res **50**:256–264, 1982.
66. Sparrow M, Arner A, Hellstrand P, Morono L, Mohammad MA, Ruegg JC. Isoforms of myosin in smooth muscle. In: Siegman MJ, Ed. The Contractile Process of Smooth Muscle. New York: Allan R. Liss Inc., 1987.
67. Mohammed MA, Sparrow MP. Changes in myosin heavy chain stoichiometry in pig tracheal smooth muscle during development. FEBS Lett **228**:109–112, 1988.
68. DeMarzo N, DiBlasi P, Milani GF, Pivirotto F, Mapp C, Sartore S, Fabbri LM. Distribution of smooth muscle myosin heavy chain (MHC) isoforms in bronchial and tracheal biopsies of asthmatic and normal subjects. FASEB J **2**:A1698, 1988.
69. Packer CS. Myosin heavy chain isoform pattern is not altered in arterial smooth muscle from the spontaneously hypertensive rat. In: Sperelakis N, Ed. Frontiers in Smooth Muscle Research. New York: Alan R. Liss, pp575–582, 1990.
70. Lema MJ, Pagani ED, Shemin R, Julian FJ. Myosin isozymes in rabbit and human smooth muscle. Circ Res **59**:115–123, 1986.
71. Eddinger TJ, Wolf JA. Expression of four myosin heavy chain isoforms with development in mouse uterus. Cell Motility Cytoskel **25**:358–368, 1993.
72. Kelley CA, Takahashi M, Yu JH, Adelstein RS. An insert of seven amino acids confers functional differences between smooth muscle myosins from the intestines and vasculature. J Biol Chem **268**:12848–12854, 1993.
73. Brutsaert DL, DeClerck NM, Goethals MA, Housmans PR. Relaxation of ventricular cardiac muscle. J Physiol **283**:469–480, 1978.
74. Johansson B, Hellstrand P. Isometric and isotonic relaxation in venous smooth muscle. Acta Physiol Scand **93**:164–167, 1975.
75. Packer CS, Stephens NL. Force-velocity relationships in hypertensive arterial smooth muscle. Can J Physiol Pharmacol **63**:669–674, 1985.
76. Brutsaert DL, Claes VA, DeClerck NM. Relaxation of mammalian single cardiac cells after pretreatment with the detergent Brij-58. J Physiol (London) **283**:481–491, 1978.
77. Murphy RA. Control of the actin-myosin interaction in vascular smooth muscle. Blood Vessels **14**:241–242, 1976.
78. Somlyo AV. Ultrastructure of vascular smooth muscle. In: Bohr DF, Somlyo AP, Sparks HV Jr., Eds. Handbook of Physiology. The Cardiovascular System. Vol. 2: Vascular Smooth Muscle. Bethesda, MD: Am Physiol Soc, pp33–67, 1980.
79. Lowy J, Mulvany MJ. Mechanical properties of guinea pig taenia coli muscle. Acta Physiol Scand **88**:123–126, 1973.
80. Cox RH. Influence of muscle length on series elasticity in arterial smooth muscle. Am J Physiol **234**(5):C146–C154, 1978.
81. Cohen ML, Berkowitz BA. Decreased vascular relaxation in hypertension. J Pharmacol Exp Ther **196**(2):396–406, 1976.
82. Packer CS, Stephens NL. Prolonged isobaric relaxation time in small mesenteric arteries of the spontaneously hypertensive rat. Can J Physiol Pharmacol **65**:230–235, 1987.
83. Mulvany MJ, Nyborg N. An increased calcium sensitivity of mesenteric resistance vessels in young and adult spontaneously hypertensive rats. Br J Pharmacol **71**:585, 1980.
84. Sherry JMF, Gorecka A, Aksoy MO, Dabrowska R, Hartshorne DJ. Role of calcium and phosphorylation in the regulation of the activity of gizzard myosin. Biochemistry **17**:4411–4418, 1978.
85. Shibata S, Kurahashi K, Kuchii M. A possible etiology of contractility impairment of vascular smooth muscle from spontaneously hypertensive rats. J Pharmacol Exp Ther **185**:406–417, 1973.
86. Hermsmeyer K. Electrogenesis of increased norepinephrine sensitivity of vascular smooth muscle in hypertension. Circ Res **38**:362–367, 1976.
87. Arner A, Uvelius B. Force-velocity characteristics and active tension in relation to content and orientation of smooth muscle cells in aortas from normotensive and spontaneous hypertensive rats. Circ Res **50**:812–821, 1982.
88. Mulvany MJ, Hansen PK, Aalkjaer C. Direct evidence that the greater contractility of resistance vessels in spontaneously hypertensive rats is associated with a narrowed lumen, a thickened media, and an increased number of smooth muscle cell layers. Circ Res **43**:854–864, 1978.
89. Roepke JE, Packer CS, Rhoades RA. Arterial myosin heavy chain isoform shifts are not primary in the etiology of hypoxia-induced pulmonary hypertension. FASEB J **5**:A403, 1991.
90. Chamley-Campbell J, Campbell GR, Ross R. The smooth muscle cell in culture. Physiol Rev **59**:1–61, 1979.
91. Seidel CL, Wallace CL, Dennison DK, Allen JC. Vascular myosin expression during cytokinesis, attachment and hypertrophy. Am J Physiol **256**:C793–C798, 1989.
92. Berner PF, Somlyo AV, Somlyo AP. Hypertrophy-induced increase of intermediate filaments in vascular smooth muscle. J Cell Biol **88**:96–101, 1981.
93. Folkow B, Hallback M, Lundgren Y, Siverston R, Weiss L. Importance of adaptive changes in vascular design for establishment of primary hypertension, studied in man and spontaneously hypertensive rats. Circ Res **32/33**(Suppl 1):2–16, 1973.
94. Sweet CS, Arbegast PT, Gaul SL, Baine EH, Gross DM. Relationship between angiotensin 1 blockade and antihypertensive properties of single doses of MK-421 and captopril in spontaneous and renal hypertensive rats. Eur J Pharmacol **76**:167–176, 1981.
95. Ebashi S. The Croonian Lecture. Regulation of muscle contraction. Proc R Soc London Ser B **207**:259–286, 1980.
96. Mulvany MJ. Lack of difference in mechanical and morphological properties of smooth muscle cells from mesenteric resistance vessels in spontaneously hypertensive and normotensive Wistar-Kyoto rats. In: Stephens NL, Ed. Smooth Muscle Contraction. New York: Marcel Dekker, 1984.
97. Packer CS, Kagan ML, Stephens NL. Decreased velocity of shortening in arterial smooth muscle from older (28–31 week old) spontaneously hypertensive rats. Can J Physiol Pharmacol **64**:96–100, 1986.
98. Alpert NR, Hamrell BB, Halpern W. Mechanical and biochemical correlates of cardiac hypertrophy. Circ Res **34/35**(Suppl 2):71–82, 1974.
99. Maughan D, Low E, Litten III R, Brayden J, Alpert N. Calcium-activated muscle from hypertrophied rabbit hearts. Circ Res **44**:279–287, 1979.
100. Brutsaert DL, Claes VA. Onset of mechanical activation of mammalian heart muscle in calcium- and strontium-containing solutions. Circ Res **35**:345–357, 1974.
101. Claes VA, Brutsaert DL. Infrared emitting diode and optic fibers for underwater force measurement in heart muscle. J Appl Physiol **31**:497–498, 1971.
102. Brutsaert DL. The force-velocity-length-time interrelation of cardiac muscle. In: Porter, R and Fitzsimons, DW, Eds. The Physiologic Basis of Starling's Law of the Heart. Ciba Foundation Symposium 24 (new series). New York: Elsevier, pp 155–191, 1974.
103. Meiss RA. Dynamic stiffness of rabbit mesotubarium smooth muscle: Effect of isometric length. Am J Physiol **234**:C14–C26, 1978.
104. Meiss RA. A versatile transducer system for mechanical studies of muscle. J Appl Physiol **37**:459–463, 1974.
105. Meiss RA. Nonlinear force response of active smooth muscle subjected to small stretches. Am J Physiol **246**:C114–C124, 1984.
106. Lash JA, Sellers JR, Hathaway DR. The effects of caldesmon on smooth muscle acto-HMM ATPase activity and binding of HMM to actin. J Biol Chem **261**:16155–16160, 1986.
107. Winder SJ, Sutherland C, Walsh MP. Biomedical and func-

tional characterization of smooth muscle calponin. In: Moreland, RS, Ed. Advances in Experimental Medicine and Biology (Regulation of Smooth Muscle Contraction). Plenum Press: New York Vol **304:** pp37–51, 1991.
108. Mulvany MJ, Baandrup U, Gundersen HJG. Evidence of hyperplasia in mesenteric resistance vessels of spontaneously hypertensive rats using a three-dimensional disector. Circ Res **57:**794–800, 1985.
109. Bagby RM. Organization of contractile/cytoskeletal elements. In: Stephens NL, Ed. Biochemistry of Smooth Muscle, Vol **1:** pp1–84, Boca Raton, FL: CRC Press, 1983.
110. Gabella G. Structural apparatus for force transmission in smooth muscles. Physiol Rev **64:**455–477, 1984.
111. Dabrowska R, Aromatorio D, Sherry JMF, Hartshorne DJ. Composition of the myosin light chain kinase from chicken gizzard. Biochem Biophys Res Commun **78:**1263–1272, 1977.
112. Adelstein RS, Eisenberg E. Regulation and kinetics of the actin-myosin-ATP interaction. Ann Rev Biochem **49:**921–956, 1980.
113. Hartshorne DJ, Gorecka A. Biochemistry of the contractile proteins of smooth muscle. In: Bohr DF, Somlyo AP, Sparks HV Jr., Eds. Handbook of Physiology. The Cardiovascular System. Vol. 2: Vascular Smooth Muscle. Bethesda, MD: Am Physiol Soc, pp 93–120, 1980.
114. Chacko S, Rosenfeld A. Regulation of actin-activated ATP hydrolysis by arterial myosin. Proc Natl Acad Sci USA **70:**292–296, 1982.
115. Nag S, Seidel JC. Dependence on Ca^{2+} and tropomyosin of the actin-activated ATPase activity of phosphorylated gizzard myosin in the presence of low concentrations of Mg^{2+}. J Biol Chem **258:**6444–6449, 1983.
116. Kaminski EA, Chacko S. Effects of Ca and Mg on the actin-activated ATP hydrolysis by phosphorylated heavy meromyosin from arterial smooth muscle. J Biol Chem **259:**9104–9108, 1984.
117. Ebashi S. Regulation of contractility. In: Stracher A, Ed. Muscle and Nonmuscle Motility. New York: Academic, Vol **1:** pp 217–232, 1983.
118. Marston SB. The regulation of smooth muscle contractile proteins. Prog Biophys Mol Biol **41:**1–41, 1982.
119. Rasmussen H, Barrett PQ. Calcium messenger system: An integrated view. Physiol Rev **64:**938–984, 1984.
120. Takahashi K, Hiwada K, Kokubu T. Isolation and characterization of a 34,000-dalton calmodulin- and F-actin-binding protein from chicken gizzard smooth muscle. Biochem Biophys Res Commun **141:**20–26, 1986.
121. Pato MD, Adelstein RS. Purification and characterization of a multi-subunit phosphatase from turkey gizzard smooth muscle. The effect of calmodulin binding to myosin light chain kinase on dephosphorylation. J Biol Chem **258:**7047–7054, 1983a.
122. Pato MD, Adelstein RS. Characterization of a Mg^{2+}-dependent phosphatase from turkey gizzard smooth muscle. J Biol Chem **258:**7055–7058, 1983.
123. Driska SP, Aksoy MO, Murphy RA. Myosin light chain phosphorylation associated with contraction in arterial smooth muscle. Am J Physiol **240:**C222–C233, 1981.
124. Aksoy MO, Mras W, Kamm KE, Murphy RA. Ca^{2+}, cAMP, and changes in myosin phosphorylation during contraction of smooth muscle. Am J Physiol **245:**C255–C270, 1983.
125. Aksoy MO, Murphy RA, Kamm KE. Role of Ca^{2+} and myosin light chain phosphorylation in regulation of smooth muscle. Am J Physiol **242:**C109–C116, 1982.
126. Arner A. Force-velocity relation in chemically skinned rat portal vein: Effects of Ca^{2+} and Mg^{2+}. Pflugers Arch **397:**6–12, 1983.
127. Paul RJ, Doerman G, Zeugner C, Ruegg JC. The dependence of unloaded shortening velocity on Ca^{2+}, calmodulin, and duration of contraction in "chemically skinned" smooth muscle. Circ Res **53:**342–351, 1983.
128. Arner A, Hellstrand P. Activation of contraction and ATPase activity in intact and chemically skinned smooth muscle of rat portal vein: Dependence on Ca^{2+} and muscle length. Circ Res **53:**695–702, 1983.
129. Krisanda JM, Paul RJ. Energetics of isometric contraction in porcine carotid artery. Am J Physiol **246:**C510–C579, 1984.
130. Chacko S, Conti MA, Adelstein RS. Effect of phosphorylation of smooth muscle myosin on actin activation and calcium regulation. Proc Natl Acad Sci USA **74:**129–133, 1977.
131. Lebowitz EA, Cooke R. Phosphorylation of uterine smooth muscle permit actin-activation. J Biochem (Tokyo) **85:**1489–1494, 1979.
132. Sobieszek A. Vertebrate smooth muscle myosin enzymatic and structural properties. In: Stephens NL, Ed. The Biochemistry of Smooth Muscle. Baltimore, MD: University Park Press, pp 413–433, 1977.
133. Bagby RM, Pepe RA. Striated myofibrils in anti-myosin stained, isolated chicken gizzard smooth muscle cells. Histochemistry **58:**219–235, 1978.
134. Sobieszek A. Ca^{2+}-linked phosphorylation of light chain vertebrate smooth muscle myosin. Eur J Biochem **73:**477–483, 1977.
135. Groschel-Stewart U, Chamley JH, McConnel JD, Barnstock G. Comparison of the reaction of cultured smooth and cardiac muscle cells and fibroblasts to specific antibodies to myosin. Histochemistry **43:**215–224, 1975.
136. Sobieszek A, Bremel RD. Preparation and properties of vertebrate smooth muscle myofibrils and actomyosin. Eur J Biochem **55:**49–60, 1975.
137. Gaylinn BG, Eddinger TJ, Martino PA, Monical PL, Hunt DF, Murphy RA. Expression of nonmuscle myosin heavy and light chains in smooth muscle. Am J Physiol **257:**C997–C1004, 1989.
138. Monical PL, Owens GK, Murphy RA. Expression of myosin regulatory light-chain isoforms and regulation of phosphorylation in smooth muscle. Am J Physiol **264:**C1466–C1472, 1993.
139. Sparrow MP, Mitchell HW, Everett AW. Different ratio of myosin heavy chain isoforms in arterial smooth muscle of the spontaneously hypertensive rats. Basic Res Cardiology **85:** 209–216, 1990.